Properties of Terrestrial Gamma ray Flashes

Modelling and Analysis of BATSE and RHESSI data

Thomas Gjesteland

Dissertation for the degree of Philosophiae Doctor (PhD)

Department of Physics and Technology
University of Bergen

April 2012

Preface

This synthesis and collection of papers are submitted for the degree of philosophiae doctor (PhD) in physics at the Department of Physics and Technology, University of Bergen.

The thesis is divided into an introductory part and a part consisting of five papers published in international peer reviewed journals.

1. Østgaard, N., T. Gjesteland, J. Stadsnes, P. H. Connell, and B. Carlson, *Production altitude and time delays of the terrestrial gamma flashes: Revisiting the Burst and Transient Source Experiment spectra*, J. Geophys. Res., 113, A02307, doi:10.1029/2007JA012618, 2008

2. Gjesteland, T., N. Østgaard, P. H. Connell, J. Stadsnes, and G. J. Fishman, *Effects of dead time losses on terrestrial gamma ray flash measurements with the Burst and Transient Source Experiment*, J. Geophys. Res., 115, A00E21, doi:10.1029/2009JA014578, 2010

3. Gjesteland, T., N. Østgaard, A. B. Collier, B. E. Carlson, M. B. Cohen, N. G. Lehtinen *Confining the Angular Distribution of Terrestrial Gamma-ray Flash Emission.*, J. Geophys. Res., 116, A11313, doi:10.1029/2011JA016716, 2011

4. Gjesteland, T.,N. Østgaard, A. B. Collier, B. E. Carlson, C. Eyles, D. M. Smith *A new method reveals more TGFs in the RHESSI data* Geophys. Res. Lett., 39, L05102, doi:10.1029/2012GL050899, 2012

5. Østgaard, N., T. Gjesteland, B. E. Carlson, R. S. Hansen, and A. B. Collier, *The true fluence distribution of terrestrial gamma flashes at satellite altitude*, J. Geophys. Res., 117,A03327, doi:10.1029/2011JA017365,

Additional papers

I have, during my Ph.D. studies, also contributed to the following papers. They are not a part of the thesis.

- Cohen, M. B., U. S. Inan, R. K. Said, and T. Gjesteland, *Geolocation of terrestrial gamma ray flash source lightning*, Geophys. Res. Lett., 37, L02,801, doi:10.1029/2009GL041753, 2010.

- Collier A. B., T. Gjesteland, N. Østgaard. *Assessing the Power Law Distribution of TGFs.*, J. Geophys. Res,116 ,A10320, doi:10.1029/2011JA016612, 2011.

- Carlson B. E., T. Gjesteland, N. Østgaard. *Terrestrial gamma ray flash electron beam geometry, fluence, and detection frequency*,J. Geophys. Res, 116, A11217, doi:10.1029/2011JA016812,2011

- Carlson B. E., T. Gjesteland, N. Østgaard. *Connecting the terrestrial gamma-ray flash source strength and observed fluence distributions*,J. Geophys. Res, Res., 116, A11217, doi:10.1029/2011JA016812,2011

Contents

List of Figures

Acknowledgements

This PhD thesis is the result of four year work at the University of Bergen. All together I have now been at the University ten years and there are many people who have helped me and supported me during those years and I am very thankful.

First I will thank my advisor Nikolai Østgaard for all the help during my master and PhD Studies. He has been an excellent advisor. His enthusiasm has been a great source for inspiration and ideas. I will also thank Emeritus Johan Stadsnes who always has an open door and have given impressive answers to my questions. I am very grateful for the help and inspiring discussion with Brant Carlson whom I shared the office with the last two years in Bergen and at the time at Stanford. Thanks to Andrew Collier whom I had the pleasure to share office with the two months he visited our group.

I spent one semester at the VLF group at Stanford University which gave me a lot of experience. I will thank Umran Inan forn for inviting me to his group, and thanks to Brant Carlson, Nikolai Lehtinen and Morris Cohen for the collaboration at Stanford.

I would like to thank David Smith for the help and the use of the RHESSI data. Thanks to Jerry Fishman for the help and use of the BATSE data and Hugh Christian for the use of LIS/OTD data. Thanks to Paul Connell for the help in analysing the BATSE data and Chris Eyles for the help in developing the RHESSI search algorithm.

The years at the Department of physics and technology have been great. Thanks to the whole Space physics group and the associated for the social events, lavvo trips, cakes and other fun. It has been an inspiring, and fruitful environment. Many thanks to the TGFs people at UB, Brant, Ragnhild, Siri, Alexander and Øystein, for many good meetings and discussions. Thanks to Kåre Njøten and Arne Solberg for sharing old stories from the department and all the other advises. Thanks to Villy for the every day morning greetings.

I want to thank my parents and family for all help and support and also for taken care of my children whenever needed.

Finally, I am very grateful to my wife Marie for all she is and to my lovely children Mathilde and Johan.

Bergen, April 2012
Thomas Gjesteland

Chapter 1

Introduction

This thesis objective is to study Terrestrial Gamma ray Flashes (TGFs), which are short burst ($\sim$ 1 ms) of gamma-radiation from thunderstorms first discovered by *Fishman et al.* [1994]. The measured photons energies in TGFs are found to be up to several tens of MeV [*Smith et al.*, 2005; *Marisaldi et al.*, 2010a], which make them the most energetic natural photon phenomenon on Earth. The physics behind the production of TGFs are not well established. TGFs are assumed to be bremsstrahlung from relativistic electrons which are accelerated in strong electric fields related to thunderstorms. However, it is not known how frequent TGFs are, what are the altitude range in which they can be produced, the spatial extent of their source region, the angular distribution of the photons at the production altitude or to what kind of thunderstorms and lightning they are related to. There is a few suggested theories of how TGFs can be produced, but there are so far no consensus.

The aim of this thesis is to study TGFs in order to understand what this recently discovered natural phenomenon is. In the papers presented in this thesis several questions regarding the nature of TGFs are addressed. The main contributions can be summarized in three points.

1) Determine the production altitude of TGFs. The production altitude will give constraints on the electric fields that produces TGF and which type of lightning and/or thunderstorms that produces TGFs. The production altitude is investigated by comparing Monte Carlo simulations with measurements from the Burst And Transient Source Experiment (BATSE). The conclusions of Paper I [*Østgaard et al.*, 2008] and Paper II [*Gjesteland et al.*, 2010] of this thesis is that the TGFs measured by BATSE are produced in $\sim 10-20$ km altitude.

2) Determine the angular distribution of the photons produced in a TGF. The distribution of emitted photons will reflect the direction of the electric fields that produces the TGFs. Paper III [*Gjesteland et al.*, 2011] argue that TGFs are emitted within a cone of $30^\circ - 40^\circ$ indicating that TGFs are produced in nearly vertical electric fields.

3) Examine how common TGFs are. When TGFs were discovered they were thought to be a rare phenomenon since they were only observed $\sim$ once a month [*Fishman et al.*, 1994]. More recent results based on more sensitive instruments have observed $\sim$ 10 TGFs a month [*Grefenstette et al.*, 2009], which is more frequent but still rare. Paper IV [*Gjesteland et al.*, 2012] describes a method to lower the sensitivity threshold for the RHESSI satellite. Applying this method has more than double the number of identified TGFs. The increase of identified TGFs indicates that so far only

the top of an 'iceberg' of TGFs are observed. Paper V [*Østgaard et al.*, 2012] use an analytical approach, by comparing the relative TGF count rates of the RHESSI and Fermi satellites, to show that one cannot reject the hypothesis that all lightning produce TGFs. If this is the case, then TGFs are a very common phenomenon which may have important impacts of the coupling between the lower atmosphere and space.

This thesis starts with a historical walk trough the TGF research starting almost hundred years ago. Chapter 3 describes the two satellites instruments, BATSE and RHESSI, which are used in the studies of this thesis. Also, a brief overview of other experiments which have measured TGFs are presented. The same chapter also describes radio measurements of lightning which are found to be associated TGFs. Chapter 4 describes the basic theory behind TGFs. In chapter 5 present a brief summary of each of five papers, which is the scientific contribution in this thesis. The five papers are presented in chapter 6.

Chapter 2

History of terrestrial gamma ray flashes

2.1 Early years

Lightning have always fascinated mankind. In ancient times lightning and thunder were described by mythological creatures such as Thunderbirds or Thor and his hammer Mjølne. The modern understanding of lightning started with the famous kite experiment by Benjamin Franklin. Two hundred and fifty years ago he flew his kite into a thunderstorm and showed that lightning is electricity.

In the early 1920 C. T. R. Wilson, the Noble prize winner for the discovery of the cloud chamber, studied the electrical field of thunder clouds [*Wilson*, 1924]. He made a very simple model where he assumed that the thundercloud is an electric dipole. Above the thunderstorm the electric force on electrons, due to the electric moment of the dipole, decreases approximately with $1/z^3$ where z is the hight above the cloud. The threshold for dielectric breakdown in air scales approximately as the densities, which, in our atmosphere, decreases exponentially with a scale hight of ~ 7 km. Therefore there will be a point above the thundercloud, estimated by Wilson to be 60 km [*Wilson*, 1924], where breakdown occurs. This was a prediction for red sprites as they are known today [*Williams*, 2010]. Red sprites are transient luminous events (TLE), caused by electrical discharges that occur above thunderclouds.

In the cloud chamber Wilson found that the ionization tracks of electrons straightened with increasing energy [*Williams*, 2010]. In other words he found that the friction force on electrons decrease at increasing energies. With an applied electric field, such as those in thunderclouds, the electric acceleration force can exceed the friction force due to collision and the electron would run away and gain energy. Wilson stated:

Thus, β-particles which have traversed a few metres in the direction of the field have already acquired energies exceeding those of the fastest known β-particles from radioactive substances. [*Wilson*, 1924, p. 37D].

Such electrons, which experience a decreasing drag force at increasing energies, are now called runaway electrons. When high energy electrons, such as those Wilson discovered in the cloud chamber, collide with air molecules they will produce bremsstrahlung. Wilson predicted:

It would be of interest to test by direct experiment whether a thundercloud does emit any measurable amount of extremely penetrating radiation of X- or γ-ray type. [*Wilson*, 1925, p. 538].

2.2 Discovery of Terrestrial Gamma Ray Flashes

66 years after Wilson's prediction the Burst and Transient Source Experiment (BATSE) on board the Compton Gamma Ray Observatory (CGRO) observed the first TGF south of India April 22, 1991 [*Fishman et al.*, 1994]. CGRO was a big NASA observatory designed to study cosmic gamma ray burst (GRB). The BATSE instrument could estimate the direction from which the GRB comes. Since some of the bursts came from the Earth at times when the CGRO was close to thunderstorms, *Fishman et al.* [1994] concluded that this was the radiation from thunderclouds predicted by *Wilson* [1925].

Figure 2.1 shows the light curve of the first TGF. It is shorter than a typical GRB and contains a harder energy spectrum. The TGFs detected by BATSE have a duration of ~ 1 ms and energies above 1 MeV [*Fishman et al.*, 1994]. BATSE measured a total of 78 TGFs during its eight years mission.

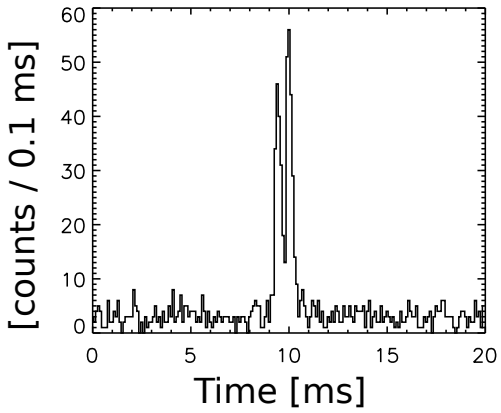

Figure 2.1: The light curve of BATSE trigger 106.

2.3 X and gamma-rays from thunderstorms

Fishman et al. [1994] was not the first to detect X-rays from thunderclouds. Wilson's ideas that thundercloud produce high energy radiation motivated several efforts to find such radiation and in the 1980-ties came the first evidence of X-rays from thunderclouds. *Parks et al.* [1981] and *Mccarthy and Parks* [1985] flew X-ray detectors in thunderclouds and found continuous X-rays with energy > 110 keV. The high X-ray fluxes lasted seconds prior to the observed lightning and returned to background within 0.1 second within the lightning discharge. They were surprised by the heigh photon fluxes and the high energies they measured. In the atmosphere there are naturally high energy particles and X-ray radiation caused by energetic cosmic rays and the extensive air showers of secondary particles they produce. E.g. [*Carlson et al.*, 2008] estimated that cosmic radiation produce $\sim 10^3 - 10^4$ energetic electrons per m^3 per second. However, *Mccarthy and Parks* [1985] concluded that their measurements of high energies and fluxes could not be described by cosmic rays alone: *An urgent problem is the iden-*

tification of the origin of the energetic electrons, whose presence is indicated by the observations presented here. Two processes meriting further study include the original Wilson mechanism and the production of energetic electrons near the concentrated field regions of leader tips. Any acceptable model must account for both the number flux and the high energies which are detected. [*Mccarthy and Parks*, 1985]

Continuous X-ray emission from thunder clouds have also been measured by *Eack et al.* [1996] who flew a balloon into a thundercloud. They measured minute long emission of X-rays which increased two orders of magnitude as the balloon passes through regions with enhanced electric field strength.

Even if the continues X-ray emissions from thunderstorms are different from TGFs in duration, fluxes and photon energies, both phenomena are assumed to origin from runaway processes.

Motivated by the observations of the high X-rays fluxes in thunderstorms *Gurevich et al.* [1992] picked up the idea of Wilson and further developed the theory of runaway electrons to runaway breakdown avalanches. The models were improved by *Roussel-Dupré et al.* [1994] with a kinetic treatment and the influence of magnetic field by *Gurevich et al.* [1996]. With the discovery of TGFs *Roussel-Dupré and Gurevich* [1996] argued that the TGF measurements by BATSE were a manifestation of relativistic runaway electron avalanches (RREA) in air. RREA is a theory that explains how discharges may occur in fields that are only one tenth of the conventional breakdown threshold. More detailed description of RREA and the production mechanisms of TGFs are presented in chapter 4.

Recent observations by satellite instruments such as Reuven Ramaty High Energy Solar Spectroscopic Imager (RHESSI) [*Grefenstette et al.*, 2009], Fermi Gamma ray Space Telescope [*Fishman et al.*, 2011] , and Astrorivelatore Gamma a Immagini Leggero (AGILE) [*Marisaldi et al.*, 2010a] have increased the knowledge about TGFs as this thesis has progressed. It is now widely accepted that TGFs occurs in RREA processes related to lightning activity. Most recent studies, included the results in this thesis, suggest that TGFs are produced below ~ 20 km, which indicates that it is electrical fields inside or right above thunderclouds that are the source of TGFs. But it is still not known how often TGFs occur and what is the driving electric field that produces them.

All instruments that have detected TGFs so far were designed for other purpose than TGFs. Therefore the measurements have certain problems. Especially deadtime losses in the measurements of the very high fluxes in TGFs have been a problem. Currently new mission, such as the Atmosphere-Space Interactions Monitor (ASIM) and Tool for the Analysis of Radiations from lightNIng and Sprites (TARANIS), are planned for space observation with electronic designed to handle the high fluxes in TGFs. These missions are needed to address the unknown questions about this very energetic natural photon phenomenon.

Chapter 3

TGF observations

This chapter will give an introduction to the measurements of TGF so far. This thesis have used data from the Burst and Transient Source experiment (BATSE) (paper I and II) and Reuven Ramaty High Energy Solar Spectroscopic Imager (RHESSI) (Paper III, IV and V). The TGF detection rate of Fermi Gamma Ray Space Telescope is used in paper V. Section 3.5 will discuss the detection of atmospherics (sferics) radio measurements which are related to TGFs. Such measurements are used in paper III and IV of this thesis.

3.1 Burst and Transient Source experiment (BATSE)

BATSE was one of four experiments on board the Compton Gamma Ray Observatory (CGRO). CGRO was a low Earth orbiting observatory ($\sim$ 450 km altitude) with inclination of 28.5°. It was launched April 5, 1991 and deliberately de-orbited on June 4, 2000. The primary objective was to study cosmic gamma ray burst (GRB), which due to the attenuation of gamma rays in the atmosphere, is not detectable on ground.

BATSE consisted of eight Sodium Iodide (NaI) Large Area Detector (LAD), each 2000 cm^2 [*Fishman et al.*, 1994] sensitive to photons with energies from 20 keV to 2 MeV [*Grefenstette et al.*, 2008]. The detectors were placed in each of the spacecraft's eight corners with the faces pointing in the same direction as in an octahedron. With this geometry one can use the ratio of counts in each detector to determine the location of the gamma source. Figure 3.1 shows the CGRO when it was launched from the Atlantis space shuttle. Four of the eight BATSE modules are marked with red circles.

To limit the amount of data BATSE used a trigger scheme to only collect the the most intense events. The search window were fixed to 64 ms, 256 ms and 1024 ms. The signal-to-noise threshold were changing during the mission but the typical trigger regime for TGFs was 5.5σ above background for a selection of the energy discriminators in the 64 ms window. 64 ms is long compared to the typical duration of TGFs ($\sim$ 1 ms). BATSE will therefore be biased to detected the longest and most intense TGFs. More description about the BATSE trigger criteria can be found at `http://gammaray.msfc.nasa.gov/batse/grb/catalog/current/trigger_criteria.html`.

The data was stored as time tagged events with time resolution of 2 μs and the energy in one of four fast discriminator channels covering the energy range $20-50$, $50-100$, $100-300$ and >300 keV [*Fishman et al.*, 1994]. The TGF energy spectra measured by BATSE were proportional to $\sim \varepsilon^{\lambda}$, where ε is the count energy and λ

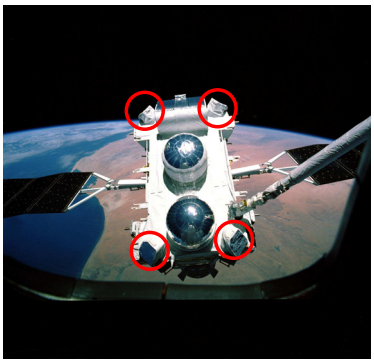

Figure 3.1: CGRO at launch from the space shuttle. Four of the BATSE LAD modules are marked with red circles. Image credit: NASA

varied from -0.6 to -1.5 [*Nemiroff et al.*, 1997]. Such energy spectra are harder than the energy spectra from GRB.

The TGFs measured by BATSE typically contain about 100 counts and have a duration $0.67 - 10.71$ ms [*Nemiroff et al.*, 1997]. The shortest TGFs consist of a single pulse, while the longer contain multiple pulses each lasting ~ 1 ms. The longest TGF, trigger 1457 (see figure 3.2), contain five pulses each separated about 2 ms [*Nemiroff et al.*, 1997]. Figure 3.2 show six examples of BATSE TGFs. Many of the TGFs measured by BATSE contains two or more pulses.

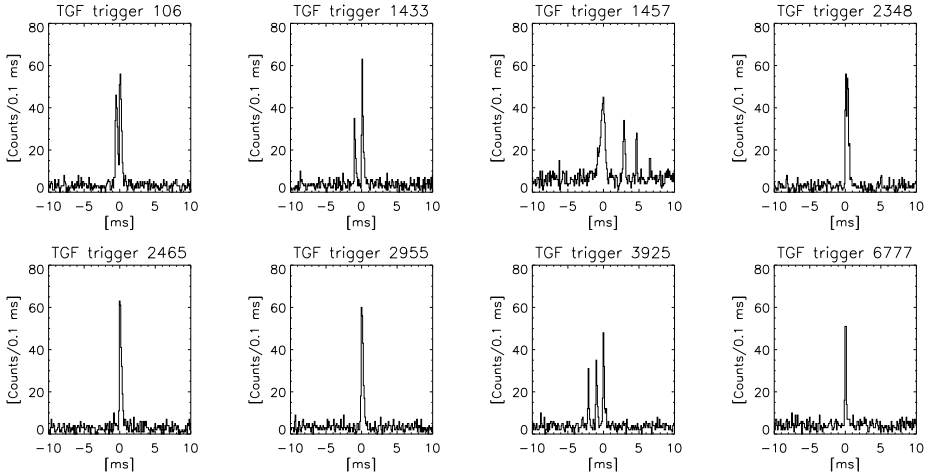

Figure 3.2: Lightcurve of BATSE TGFs. Many of the BATSE TGFs contained multiple pulses e.g. trigger 106, 1433, 1457 and 3925.

During its lifetime BATSE detected 78 TGFs [`http://gammaray.msfc.nasa.gov/batse/misc/triggers.html`]. Among the 78 TGFs from BATSE *Dwyer* [2008] suggested that many of them are in fact not burst of gamma, but bursts of electrons and

positrons. A further discussion on electrons beams produced by TGFs can be found in section 4.6.

The first analysis of the BATSE TGF data found a minimum variability time scale of typical 50 μs and interpreted this as TGFs were produced over a 15 km (50 μs $\times$ the speed of light) long region [*Nemiroff et al.*, 1997]. This finding together with the assumption that the atmosphere is only transparent for gamma-rays at altitudes above 40 km led to the conclusion that BATSE TGFs were related to red sprites.

Carlson et al. [2007] used a superposed spectrum from all the BATSE TGFs and compared it to simulated spectra. They found that a production altitude of 15-20 km could best represent the data. In paper I of this thesis [*Østgaard et al.*, 2008] a Monte Carlo code to simulate TGFs through the atmosphere is presented. The simulations is, for the first time, compared with individual TGF measurements from BATSE. *Østgaard et al.* [2008] determined that most TGFs are produced at low altitude (< 20 km), consistent with the earlier results [*Dwyer*, 2005; *Carlson et al.*, 2007], but they also found that a significant portion came from higher altitudes ($30 - 40$ km). However, it has been shown that the BATSE instrument suffered from a significant dead-time problem [*Grefenstette et al.*, 2008], i.e., that the read-out electronics of the BATSE instruments are not fast enough to count all the scintillation pulses from the detector material (See section 3.1.1 and paper II [*Gjesteland et al.*, 2010] for more information). When the effects of dead-time were treated properly *Gjesteland et al.* [2010] showed that the TGFs *Østgaard et al.* [2008] suggested were produced at 30-40 km in fact were produced at lower altitudes.

Another interesting finding in the BATSE data is the dispersion signature in the TGFs. *Feng et al.* [2002] found that the count profile for low energy photons (20-50 keV) where shifted with respect to the higher energy photons (>300 keV) with 240 μs on average. In the simulations by *Østgaard et al.* [2008] the dispersion signature was explained as a pure Compton effect. Photons that travel through the atmosphere are Compton scattered. Compton scattering changes the photons direction and reduces its energy. As a consequence the photons that escapes the atmosphere at low energy are more scattered and therefore have gone a longer path on their way through the atmosphere. Since all photons travel with the speed of light, low energy photons will arrive satellite altitudes later than high energy photons. The dispersion found in *Østgaard et al.* [2008] was ~ 100 μs which is shorter than found in *Feng et al.* [2002]. However, as shown in *Gjesteland et al.* [2010], this difference is explained by the losses due to dead-time in the BATSE instrument.

3.1.1 Losses due to dead-time

In an analysis of count rates in both RHESSI and BATSE *Grefenstette et al.* [2008] showed that BATSE TGFs had a lower peak count rate than RHESSI TGFs when the effective detection areas were accounted for. This suggest that BATSE suffered from losses due to dead-time in the read out electronics. By analysing the BATSE preflight data *Grefenstette et al.* [2008] found that the BATSE detectors worked as paralyzable detectors. A paralyzable detector with dead-time, τ, which do not vary on the photons energy, suffers from dead-time losses on the form

$$m = ne^{-n\tau}\,, \tag{3.1}$$

where m is the measured count rate, n is the incoming pulse rate and τ is the instrument dead-time [*Knoll*, 1989]. When $n \to \infty$ the measured count rate , $m \to 0$ and the detector is totally paralyzed.

The BATSE dead-time was dependent on photon energy. As found by *Grefenstette et al.* [2008], the dead-time in BATSE can be described by

$$\tau = \alpha \ln \frac{E_p}{E_0} , \tag{3.2}$$

where α is the signal decay time, E_p is the energy of the incoming photon and E_0 is the instrument reset level. Based on preflight data the estimated values are $\alpha = 0.75\mu$s and $E_0 = 5.5$ keV [*Grefenstette et al.*, 2008]. The result of equation 3.2 is that high energy photons results in longer dead-time than lower energy photons such that the dead-time losses are more significant for harder spectra.

With the claim that BATSE peak count rate is ~ 4 times larger than measured and that the energy spectrum were changed by the losses due to dead-time [*Grefenstette et al.*, 2008], all result based on BATSE spectra were questionable. *Østgaard et al.* [2008] did spectral analysis of individual BATSE TGFs and concluded that most of the TGFs were produced at altitudes below ~ 20 km. However, a significant portion were suggested to be produced at a higher altitude ($30 - 40$ km). All of these where single pulse TGFs with high count rates indicating that these TGFs suffered the most from losses due to dead-time. Therefore *Gjesteland et al.* [2010] implemented the dead-time effects on the BATSE instrument and applied them on the single pulse TGFs. The main effects of dead-time losses for BATSE are that the energy spectrum become significantly softer for increasing losses. Such softening influence the spectral analysis of the event and, as showed in *Gjesteland et al.* [2010], the production altitude becomes lower when dead-time are treated properly. *Gjesteland et al.* [2010] conclude that also the single pulse TGFs are consistent with a production altitude below ~ 20 km altitude.

Since BATSE was a paralyzable detector a single pulse TGF can be measured as a double pulse TGF. BATSE trigger 2348 is such example. *Gjesteland et al.* [2010] suggest that this TGF contains two pulses due to paralyzation of the read-out electronics. In that case the event is ~ 6 times brighter than measured [*Gjesteland et al.*, 2010]. A full description of the dead-time effects in BATSE can be found in paper II of this thesis.

3.2 Reuven Ramaty High Energy Solar Spectroscopic Imager (RHESSI)

RHESSI (figure 3.3) is a small observatory designed to study solar flares. It was launched on February 5, 2002 into a low orbit (~ 600 km altitude) with inclination 38° and is still operating. Its instrument consists of nine Germanium detectors inside an Aluminium cryostat. The Germanium detectors are divided into front and rear segments. The front segments are used to image solar flares from the sun with an energy range of 3 kev - 2.7 MeV and is not used in search for TGFs [*Grefenstette et al.*, 2009]. The rear detectors views the whole sky and are only shielded by the thin cryostat. The rear segments energy range is ~ 30 keV to 17 MeV. If a photon deposit more than 17 MeV in one detector the photon will be measured in an overflow channel. One photon can also deposit energy in more than one detector by Compton scattering. In that

case the two (or more) counts will have the same time tag. By combining coincident counts *Smith et al.* [2005] showed that RHESSI is measuring TGFs with energy up to 20 MeV. This is a very important results since the measurements from BATSE could only tell that TGFs contains photons with energy above > 1 MeV. RHESSI has also a much higher detection rate than BATSE. The first 183 days they measured 83 TGFs [*Smith et al.*, 2005], which lead to an estimate of ~ 50 TGF per day globally. These new measurements shows that TGFs are a much more common and powerful phenomenon than previously assumed.

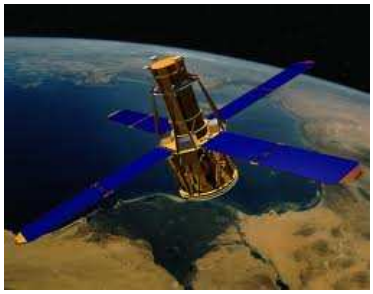

Figure 3.3: Illustration of RHESSI. Image credit: NASA.

The RHESSI relative time resolution is 1 binary micro second (2^{-20}s), but is not clear how well RHESSI are synchronised with Universal Time (UT). A giant flare from SGR 1806-20 on December 27 2004 which was measured by both the Swift and RHESSI satellites indicates that the RHESSI clock is 1.8 ms slower than UT [*Grefenstette et al.*, 2009]. It is not known if this offset is constant or varying during the mission.

Unlike BATSE RHESSI do not work in a trigger scheme but telemeters all data to ground. However, the data stream is decimated or switched off as RHESSI passes in regions with high fluxes of energetic particles such as the South Atlantic Magnetic Anomaly (SAMA), and at high latitudes where RHESSI passes close to the radiation belt.

The RHESSI catalog of TGFs is presented in *Grefenstette et al.* [2009]. It contains 820 TGFs from the period March of 2002 through February of 2008 and is the largest database of TGF events so far. The search algorithm applied on the raw data require at least 12σ above background in a 1 ms window, where the average background rate, N, is 2 counts per ms and $\sigma = \sqrt{N+1}$. This criteria is chosen such that the catalog is as clean as possible rather than complete. A typical RHESSI TGFs contains ~ 25 counts per TGF, which is significantly fewer than a typical BATSE TGF. This is due to a smaller effective detection area in RHESSI, but also due to the trigger algorithm on BATSE, which were biased to more intense events.

Grefenstette et al. [2009] also presented the results from an alternative TGF search algorithm. The number of events and quality of this search were not discussed, but it clearly showed that there are more TGFs than presented in the catalog. Motivated by these findings *Gjesteland et al.* [2012] developed a new search algorithm which was applied to the raw RHESSI data for 2004-2006. This algorithm more than doubled

the number of identified TGFs for this period. A full description and the result of this search algorithm can be found in paper IV of this thesis.

Figure 3.4 shows examples of RHESSI TGF lightcurves. Figure 3.4 a) and d) are RHESSI TGFs presented in the RHESSI catalog [*Grefenstette et al.*, 2009] and figure 3.4 b), c) ,e) and f) are new TGFs identified by the new search algorithm [*Gjesteland et al.*, 2012]. Multiple pulse TGFs such as shown in figure 3.4 d) and e) are rare in the RHESSI catalog compared to BATSE. This is most likely the result of BATSE trigger algorithms which were biased to detecting longer long events.

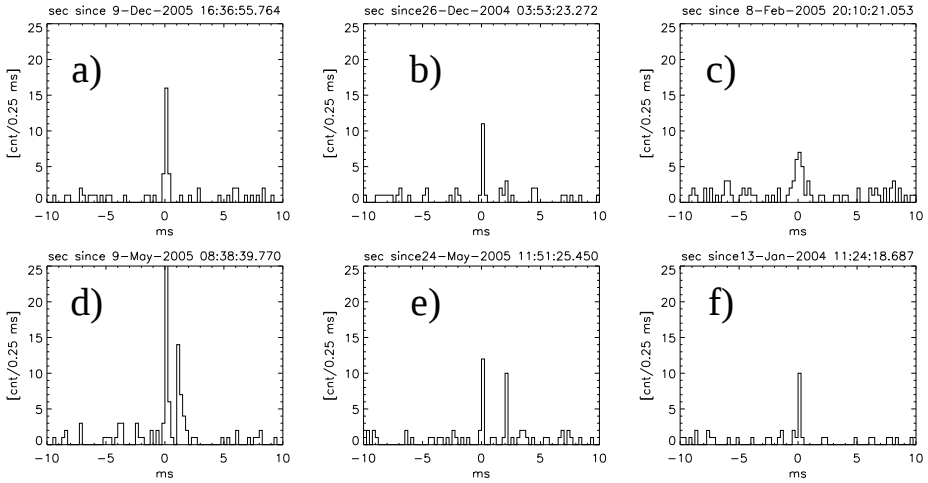

Figure 3.4: Lightcurve of RHESSI TGFs. a) and d) are RHESSI TGFs presented in the RHESSI catalog [*Grefenstette et al.*, 2009]. b), c) ,e) and f) are new TGFs identified by a new search algorithm presented by *Gjesteland et al.* [2012]

The first spectral analysis of RHESSI TGFs was done by *Dwyer and Smith* [2005]. They used a superposed spectrum of RHESSI TGF which were compared to Monte Carlo simulations. Their conclusion is that the superposed RHESSI spectrum is consistent with a source range of $15 - 21$ km, which is lower than previously assumed. These results were later confirmed by *Carlson et al.* [2007]. These new results with a production altitude below ~ 20 km points towards the cloud tops and not red sprites as the source for TGFs. *Cummer et al.* [2005] linked the RHESSI measurements to intra cloud (IC) lightning (See section 3.5), and *Williams et al.* [2006] used the properties of gamma attenuation as well as the polarity properties of lightning to support this production altitude.

Hazelton et al. [2009] identified thunderstorms near the RHESSI sub-satellite point at the time TGFs were observed. By superposing the spectrum of TGFs which had a thunderstorm within 300 km of the sub-satellite point (close events) and compare it with the superposed spectrum of TGFs without thunderstorms within 300 km (distant events), *Hazelton et al.* [2009] found that the spectrum of the distant events are softer. This is in agreement with the simulation results from *Østgaard et al.* [2008] as well as BATSE measurements which were softer at increasing observation angle [*Østgaard et al.*, 2008]. In order to determine the spatial distribution of TGF emission *Hazelton*

et al. [2009] compared the superposed spectra (close and distant) to Monte Carlo simulations. They concluded that either an emission within a narrow cone at 21 km altitude or an emission within a wide cone at 15 km altitude could best represent their measurements. Paper III *Gjesteland et al.* [2011] have addressed the same question by using RHESSI TGFs which are exactly geolocated. *Gjesteland et al.* [2011] found the same softening for distant TGFs and therefore conclude that the photons in a TGF are emitted within a cone with half angle of $\sim 30^\circ - 40^\circ$. This is in agreement with emission within the narrow cone as described by *Hazelton et al.* [2009].

Figure 3.5 shows the location of RHESSI TGFs from 2004-2006 divided into seasons. The red circles are from *Gjesteland et al.* [2012] and the green dots are TGF presented in the catalog TGFs. The grey scale is lightning activity measured by the Lightning Imaging Sensor (LIS) and Optical Transient Detector (OTD), which are optical instruments that measures lightning flashes from space [*Christian*, 2003]. The dashed lines are the limits of the RHESSI orbit. There are no TGFs in most of South America since RHESSI does not provide data for this region (SAMA). The distribution of TGFs follows the seasonal variation in lightning activity. For example during the northern hemisphere winter only one TGF occurs over the Caribbean while the vast majority of TGFs in the Caribbean occur during the northern hemisphere summer and fall.

The relation between RHESSI TGFs and lightning is also studied by *Splitt et al.* [2010]. They used data from WWLLN to identify storms related to RHESSI TGFs. The analysis shows that the TGFs are both spatially and temporally correlated with tropical thunderstorm systems. By comparing the RHESSI TGFs to the average tropopause pressure *Smith et al.* [2010] found that RHESSI TGFs tend to occur in times and places when the tropopause is high. Lightning have the same behaviour, but since the TGFs measured by RHESSI are shifted to even higher tropopause altitude it indicates that RHESSI is only detecting the TGFs that are produced at high altitude. There may be more events that are produced at lower altitude, but they are, due to atmospheric attenuation, too weak to be detected from space.

3.2.1 RHESSI dead-time

Grefenstette et al. [2008] found that both BATSE and RHESSI saturates from losses due to dead-time when they measure the high fluxes of photons in TGFs. RHESSI is a semi paralyzable detector and work as follows. If the time between two counts is less than 0.84 μs they are combined into one count (pile-up). If the time is greater than 0.84 μs and less than 5.6 μs both counts are removed by the veto system. If the time is between 5.6 μs and 9.6 μs the first count is recorded while the second is removed [*Grefenstette et al.*, 2009].

In order to determine the true TGF intensities distribution *Østgaard et al.* [2012] implemented the RHESSI dead-time effects in a Monte Carlo simulation. An example is shown in Figure 3.6. This is a TGF observed on November 26, 2004. The paralyzation curve is obtained by increasing the number of photons into a Monte Carlo simulation of the RHESSI response. The photons are distributed as a Gaussian within the estimated duration of the TGF, which for the TGF in figure 3.6 was 0.290 ms. As the number of incoming photons increase the measured count rate starts to deviate from the one-to-one relation. Simulation of a specific number of incoming photons was repeated 100

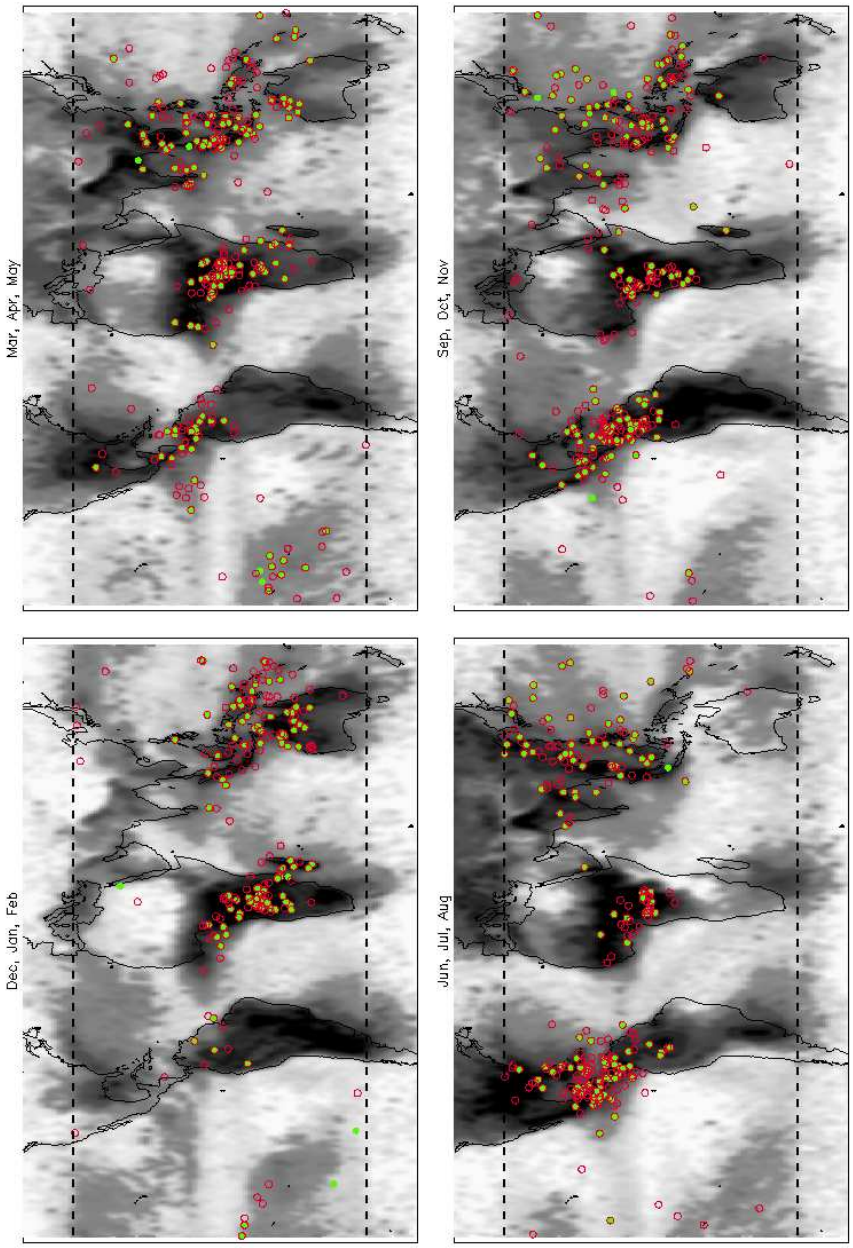

Figure 3.5: RHESSI TGFs for the years 2004, 2005 and 2006. The red circles are the TGFs found with the new search algorithm and green dots are the TGFs from the RHESSI TGF catalog. There are no TGFs in most of South America since RHESSI does not provide data for this region (SAMA). The grey scale indicates lightning activity measured by LIS/OTD. The dashed lines are the limits of the RHESSI 38° inclination orbit.

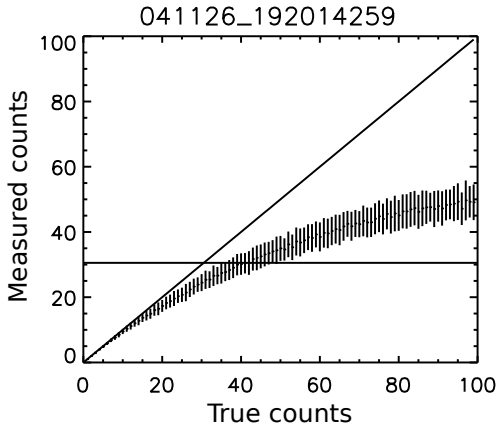

Figure 3.6: Monte Carlo simulation of the dead time losses of TGF November 26, 2004. The TGF duration is 0.290 ms. The vertical line is the number of measured counts by RHESSI. The tilted line shows the relation between measured and true counts without losses.

times to estimate the errors. The TGF in figure 3.6 contained 31 counts. By calculating where this line (31 counts) crosses the paralyzation curve this TGF is estimated to contain between 38 and 50 counts in the detectors, of which only 31 are recorded by the read-out electronics.

Østgaard et al. [2012] found that, due to the semi paralyzable behaviour, RHESSI is never totally paralyzed and it is very unlikely for RHESSI to measure a single pulse TGF as a double pulse TGF as *Gjesteland et al.* [2010] suggest BATSE did. Also, RHESSI does not have an energy dependency on the dead-time losses such as BATSE. It is therefore likely to assume that the dead-time losses in RHESSI do not influence the spectral analysis. This is also strengthened by the spectral analysis from BATSE and RHESSI that both suggest that TGFs are produced below $\sim$ 20 km altitude.

3.3 Fermi Gamma Ray Space Telescope

Fermi Gamma Ray Space Telescope (figure 3.7) was launched June 11, 2008 into a low earth orbit ($\sim$ 560 km altitude) with an inclination of 25.6° and it's primary objective is to study GRB [*Briggs et al.*, 2010]. It consists of two instruments; the Large Area Telescope (LAT) and the Gamma-ray Burst Monitor (GBM). So far only GBM have been used to identify TGFs. GBM has 12 NaI scintillator detectors with energy range $\sim$ 8 keV to 1 MeV and two Bismuth Germanate (BGO) scientillator with energy range $\sim$ 200 keV to $\sim$ 40 MeV [*Briggs et al.*, 2010]. Like BATSE, Fermi GBM has an on-board trigger algorithm. It triggers when the count rate is significant above background. The time scale and energy range can be modified in the flight software.

Fermi has an on board link to GPS to achieve very precise timing [*Connaughton et al.*, 2010]. The relative data time resolution is 2 μs. By a temporal analysis of the Fermi TGFs *Fishman et al.* [2011] found that the durations of the TGFs could be as short as $\sim$ 0.05 ms with rise times down to $\sim$ 10 μs. If one assume the speed of light

Figure 3.7: Illustration of Fermi Gamma Ray Space Telescope . Image credit: NASA.

this constrains the source region to ~ 2 km [*Briggs et al.*, 2010].

Fermi is still operating and recently the Fermi team has started to download all data from the regions where most TGFs are produced. By doing a ground search 234 TGFs were identified in 591.8 houers of data [*Briggs*, 2011]. This is ten times more TGFs than found in the trigger mode. This TGF count rate are used in paper V to estimate the true TGF fluence distribution as seen from space.

3.4 Astrorivelatore Gamma a Immagini Leggero (AGILE)

AGILE was launched April 23, 2007 into a low Earth orbit (~ 550 km altitude) with an inclination of 2.5° *Marisaldi et al.* [2010a]. It is sensitive to photons in the range 0.35–100 MeV. The Mini-Calorimeter (MCAL) instrument has an average detection rate of 10 TGFs/month [*Fuschino et al.*, 2011]. The first results showed TGFs with energies up to 40 MeV [*Marisaldi et al.*, 2010a], and later results indicate that TGFs can have energies up to 100 MeV [*Tavani et al.*, 2011]. The spectrum from the events with very high photon counts do not have the exponential fall off at higher energies, which the modelling results from RREA predicts. Instead the spectrum seems to have a broken power law shape. with $dn/d\varepsilon \sim \varepsilon^{-0.5\pm0.1}$ for 1 MeV $< \varepsilon <$ 7.1 $\pm$ 0.5 MeV and $dn/d\varepsilon \sim \varepsilon^{-2.7\pm0.1}$ above [*Tavani et al.*, 2011].

The AGILE MCAL has located 8 TGFs with gamma-ray photons of energies above 20 MeV with an accuracy of $\sim 5° - 10°$. All these events occurred within 600 km of the AGILE sub-satellite point [*Marisaldi et al.*, 2010b].

The small inclination orbit of AGILE results in high exposure time in the tropical region where the lightning density is the highest. *Fuschino et al.* [2011] found geographical differences in the TGF to lightning correlation which suggests that there are geographical and climatological modulation in the processes of TGF production. If one assumes that the TGF/lightning flash ratio holds at all latitudes *Fuschino et al.* [2011] estimate a global rate of 220 - 570 TGFs per day.

3.5 Sferics measurements

When TGFs were discovered they were found to occur in association with thunderstorms [*Fishman et al.*, 1994]. Lightning produce strong radio atmospheric (sferics) in

the Extremely Low Frequency (ELF < 3 kHz) and Very low Frequency (VLF, $3 - 30$ kHz) frequency range [*Rakov and Uman*, 2003, p.443]. ELF and VLF radio waves propagates well in the Earth-ionosphere wave guide with only a few dB attenuation per Mm and can therefore be detected far away from the lightning [*Cohen et al.*, 2010b]. Triangulation of sferics from several stations can be used to estimate the lightning location. It is assumed that the TGFs originate at the same location as the sferics [*Cummer et al.*, 2005; *Cohen et al.*, 2010b; *Collier et al.*, 2011; *Gjesteland et al.*, 2011].

In paper II of this thesis data from the World Wide Lightning Location Network (WWLLN) and the Atmospheric Weather Electromagnetic System for Observation, Modelling, and Education (AWESOME) network are used to calculate the distance between RHESSI sub-satellite point and the location of the source lightning. This distribution was then compared to Monte Carlo simulation of TGFs to constrain the initial angular distribution of the TGF emission [*Gjesteland et al.*, 2011].

In paper IV of this thesis [*Gjesteland et al.*, 2012] the matches between WWLLN and TGFs is also used to verify the new search algorithm on the RHESSI data. WWLLN is an expanding network which consisted of 38 stations in 2009 [*Abarca et al.*, 2010] and currently of more than 50 broadband receivers all over the world [`http://www.wwlln.net`]. It uses Time of Group Arrival (TOGA) algorithm to triangulate the source position of the emitted sferic. The quality of the network is improving due to adding more stations and improving the algorithm. In 2008-2009 WWLLN detected $\sim 10\%$ of cloud to ground (CG) lightning with currents stronger than 35 kA [*Abarca et al.*, 2010]. WWLLN has temporal and spatial accuracies of $\sim 30\ \mu$s and 10 km [*Rodger et al.*, 2005].

Connaughton et al. [2010] searched for correlation between TGFs detected by Fermi GBM and sferics measured by WWLLN and found 15 good matches of 50 available TGFs. In 13 of these TGFs the lightning were simultaneous to $\sim 40\ \mu$s of the peak of the the TGF. *Collier et al.* [2011] search for correlation between RHESSI TGFs and WWLLN and found 93 matches of 972 available TGFs. In the 93 matches *Collier et al.* [2011] found that the TGFs were preceding the associated lightning events with a mean of 0.77 ms. This suggest that the TGFs are produced in the initial stage of the lightning discharge. However, one also needs to consider that the timing of the RHESSI clock, which may not be constant, and an uncertainty of 2 ms should be included [*Grefenstette et al.*, 2009]. However, the results from *Collier et al.* [2011] indicate a systematic, rather than a random timing uncertainty.

Figure 3.8 shows the distance between the source lightning and the RHESSI sub-satellite point for the 93 TGFs which were found by *Collier et al.* [2011]. Most of the TGFs were observed closer than 400 km from the sub-satellite point but there are some events located as far as ~ 800 km away.

An interesting result from *Collier et al.* [2011] is that the matched TGFs were from the weaker end of the TGF intensity distribution. This result were further strengthen by a comparable match percentage in the new RHESSI TGFs found by *Gjesteland et al.* [2012], which contains TGFs weaker than in the RHESSI TGF catalog.

AWESOME uses wire-loop antennas which are sensitive to the orthogonal magnetic field and it is operating in the VLF range [*Cohen et al.*, 2010a]. It uses a similar technique as WWLLN to determine the source of the spheric but it also include magnetic direction finding. AWESOME have nine sites [*Cohen et al.*, 2010b] and is only sensitive to lightning from the Americas and West Pacific. A full description of AWESOME

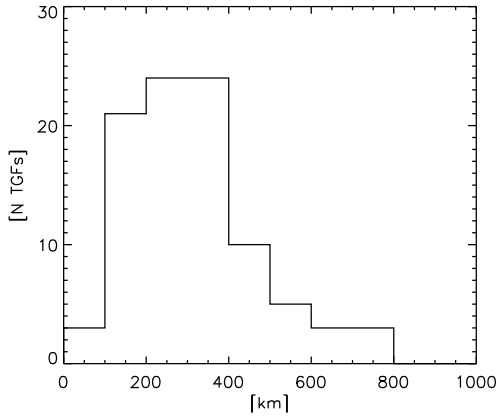

Figure 3.8: Distribution of distances between RHESSIsub-satellite point and the source lightning from WWLLN. The figure contains 93 TGFs presented in *Collier et al.* [2011].

can be found in *Cohen et al.* [2010a].

In the study by *Cohen et al.* [2010b] 36 RHESSI TGFs were geolocated, 16 of these were geolocated with measurements from 3 or more stations and they have and uncertanty in the geolocation of ~ 30 km [*Cohen et al.*, 2010b]. The two-stations cases have larger uncertainties and were not used in Paper III [*Gjesteland et al.*, 2011].

The first study indicating that there is a connection between sferics and TGFs was done by *Inan et al.* [1996] who found that two BATSE TGFs occurred in association with lightning activity. For one of the TGF their detector observed a sferic within ± 1.5 ms of the TGF. *Cohen et al.* [2006] found six additional BATSE TGFs showing a clear relation between sferics and TGFs. By studying 116 RHESSI TGFs *Inan et al.* [2006] found that 24% did not have associated sferics. However, several of these TGFs were later rejected as false events, and in a later study *Cohen et al.* [2010b] found that only 9 out of 158 TGFs are not associated with sferics. The remaining nine TGFs could be statistical anomalies or they could be associated with lightning which emits sferics below the detection threshold.

Meanwhile *Cummer et al.* [2005] compared RHESSI TGFs to sferics and found thirteen TGFs occurring within $-3/+1$ ms of a lighting discharge. All these lightning were of positive polarity. They calculated mean charge moment change to the lightning strokes associated with the TGFs to be 49 Ckm. Six of eight available RHESSI TGFs were linked to positive IC lightning by the Los Alamos Sferic Array (LASA) stations by *Stanley et al.* [2006] clearly showing that IC lighting is related to TGFs. A similar study of nine additional RHESSI events and LASA measurements also found that IC lightning and TGFs are closley related [*Shao et al.*, 2010].

In a study using the North Alabama Lightning Mapping Array (LMA) *Lu et al.* [2010] found a RHESSI TGF which were produced in association with an upward propagating leader. This TGF was followed by a slow pulse in the Ultra Low Frequency (ULF, $< 0.1 - 400$ Hz) range. The same slow pulse ($\sim 2 - 6$ ms) were found in 54 of 56 RHESSI TGFs for which the magnetic broad band data (< 0.1 Hz -30 kHz) were analysed [*Lu et al.*, 2011]. More recently *Cummer et al.* [2011] presented

two cases where a shorter, ($\sim 50\ \mu$s) but still slow, pulse in the broadband magnetic data that have a strong temporal connection with the gamma-ray count rate from Fermi GBM. Both the magnetic field data and the Fermi GBM data have very precise timing. It therefore indicates that the slow pulse and the TGF are simultaneously. However, *Cummer et al.* [2011] did not conclude whether or not the slow pulse is driven by lightning processes or by the RREA itself. However, *Dwyer* [2012] suggests that this slow pulse is emitted by the TGF producing electron avalanche as predicted by the relativistic feedback discharge (RFD) model of TGF. The RFD model is further discussed in section 4.4.3.

Chapter 4

Terrestrial gamma ray flashes

TGFs are a short flash of gamma radiation produced by thunderstorms. Based on average RHESSI TGF fluence the number of bremsstrahlung producing relativistic electrons at the production altitude must be on the order of $> 10^{16} - 10^{18}$ depending on the production altitude [*Dwyer and Smith*, 2005]. The energy of the electrons must be larger than the highest photon energy measured in TGFs, which is several tens of MeV [*Smith et al.*, 2005; *Marisaldi et al.*, 2010a]. This chapter will give a short introduction to how runaway electrons can be accelerated to relativistic energies and how a runaway avalanche can form. This chapter will also give an introduction to thunderstorms properties and discuss the theories that are suggested to explain TGF production. In section 4.5 a discussion of how these theories relates to the observations are presented, and section 4.6 gives a short introduction to electrons beams which are made by TGFs.

4.1 Runaway electrons

TGFs are assumed to be bremsstrahlung from relativistic electrons. To accelerate electrons to such high energies in the Earth atmosphere implies a runaway process. In a sufficiently large electric field energetic electrons will gain energy at a higher rate than they lose energy due to ionizing and radiation. As a results the energy of the electrons will increase and the electron becomes a runaway electron. As already known by the time C.T.R Wilson did his experiments, an electron with energy, ε, which collide with an electron or atom can be described as a Coulomb collision. The scattering from such collisions have a cross section, σ, given by $\sigma \propto 1/\varepsilon^2$. The friction force, F_D, on the electron is given by $F_D \propto \varepsilon\sigma\rho$, where ρ is the density. If one apply an electrical field, $E > F_D(\varepsilon)/q$, where q is the charge of the electron, the electrons will gain more energy than they loose due to collisions. This is the concept of runaway electrons which *Wilson* [1924] used to predict X and gamma radiation from thunder clouds.

Figure 4.1 shows the rate of energy loss of an energetic electron in a standard temperature and pressure (STP) atmosphere as a function of electron energy. This energy loss is the effective friction force, F_D on the electrons. The acceleration force on an electron due to an electric field is given by $F_a = qE$, where E is the electrical field strength and q is the electron charge. For electrons with energy ~ 1 MeV there is a minimum in the friction force and the break even electrical field $E_t \sim 2$ kV/cm, which is when $F_D = F_a$. As seen in figure 4.1 the break even field is far less than the conventional breakdown threshold in air ($E_k \sim 32$ kV/cm) and also lower than the threshold for

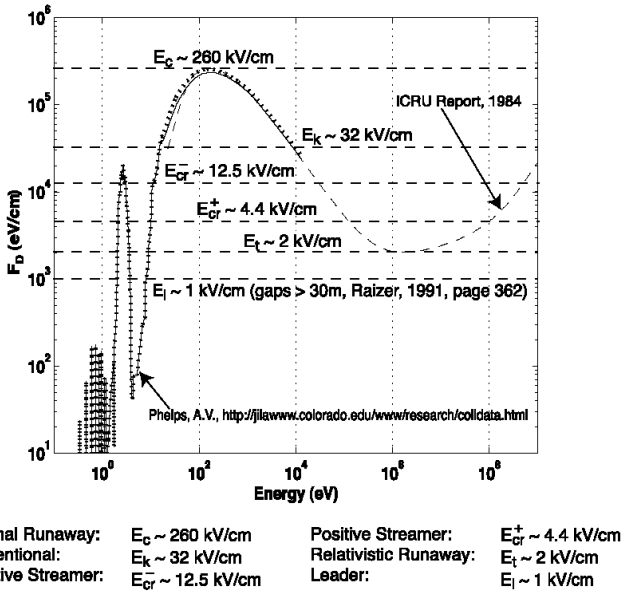

Figure 4.1: The friction force on electrons in air in a STP atmosphere. The figure is from *Moss et al.* [2006].

negative ($E_{cr}^- \sim 12.5$ kV/cm) and positive ($E_{cr}^+ \sim 4.4$ kV/cm) streamers to propagate. If the electric field is larger than $E_c \sim 260$ kV/cm thermal electrons will be accelerated over the peak in the friction force, which occur at electron energies ~ 200 eV, and into the runaway regime. This process is called cold runaway acceleration and is further discussed in section 4.4.4

It is worth to mention that runaway electrons have an upper energy limit. As the electrons energy increase the cross section for radiation increase and hence the friction fore increase. For example if the electrical field is 4.4 kV/cm the highest energy one can accelerate runaway electrons to is ~ 100 MeV (Se figure 4.1).

4.2 Relativistic runaway electron avalanche (RREA)

In strong electric fields an avalanche of runaway electrons can be formed. If the electric field accelerates an electron to such energies that it remains in the runaway regime after hard elastic scattering with atomic electrons, it is a runaway electron. If now the bounded electron gets knocked off and gain an energy such that both the runaway electron and the knock off electron are in the runaway regime after collision one gets avalanche formation. Motivated by the idea from *Wilson* [1924] and the measurements from *Mccarthy and Parks* [1985], *Gurevich et al.* [1992] studied these processes theoretical and found that relativistic runaway electron avalanche (RREA) can occur in thunderstorms. The threshold for a RREA to develop is $\sim$ 3kV/cm in STP air [*Dwyer*, 2012], which is appropriately ten times less field strength than needed for conventional

breakdown in air and 100 times less than cold runaway threshold. The RREA threshold scales with the densities which, in the atmosphere, decreases almost exponentially with an scale hight of ~ 7 km.

To initiate RREA one need seeds electrons which are in the runaway regime. In a thundercloud such electrons are constantly produced as secondary particles from cosmic rays [*Gurevich et al.*, 1992].

The avalanche growth factor, which is the number of particles one seed electron produce through the avalanche region, is highly dependent on the electrical field strength. According to [*Dwyer*, 2007, eq. 15] one can approximate the growth factor, N_{re}, by

$$N_{re} = \exp\left(\int_0^L \frac{dz}{\lambda}\right), \tag{4.1}$$

where λ is the avalanche length and L is the length of the avalanche region. For the Earth's atmosphere [*Coleman and Dwyer*, 2006, eq. 2] have estimated λ to

$$\lambda = \frac{7300 \pm 60\text{kV}}{E - 276 \pm 4\text{kV/m}} \tag{4.2}$$

solving 4.1 yields

$$N_{re} = \exp\left(\frac{E - 276\text{kV/m}}{7300\text{kV}} \times L\right). \tag{4.3}$$

In table 4.2 N_{RE} and L are calculated for various electric field strength, E and total available potential, $U = EL$. The numbers are presented are for STP air at sea level. At an altitude z the electric field scales with $n(z)/n_0$ and the length scales with $n_0/n(z)$, where n_0 is the density at sea level and $n(z)$ is the density at altitude z. The electrical fields in table 4.2 are chosen such that the electric field is larger than the RREA threshold, $E_t = 3 \times 10^5$ V/m for STP air, and lower than the conventional breakdown threshold, $E_K = 3.2 \times 10^6$ V/m for STP air. The numbers in table 4.2 shows that for total available potentials ≤ 100 MV the maximum growth factor $N_{RE} < 10^6$, while for electric fields close to the conventional breakdown threshold and total potential of 400 MV the growth factor can be $> 10^{21}$. However, there are no measurements that supports that one can have such large electric fields and potentials inside thunder clouds. Most measurements of the voltage in a thundercloud concludes that the maximum potential in a thunder cloud is in the order of ~ 100 MV [*Marshall and Stolzenburg*, 2001], however one can not exclude that higher potential exists. More discussion about thunder cloud electric fields and potential are presented in section 4.3.

If we assume that the maximum potential in a thundercloud is ~ 100 MV one sees that the maximum growth factor in RREA is $N_{RE} < 10^6$. This is far from the required $10^{16} - 10^{18}$ electrons which is needed to produce a TGF detectable in space. Therefore a model that explains TGFs must either relay on seed particles or an additional growth such as feedback first suggested by *Dwyer* [2003].

As discussed in the section above, to produce a TGF one either needs very strong electric field and high potential or additional seeding to gain the high fluence. Section 4.3 will present typical conditions in thunderstorms, and then section 4.4 will discuss the proposed theories for TGF production.

Table 4.1: The maximal growth rate, N_{RE}, and avalanches length, L, for STP air for various electric fields and total potentials. At an altitude z the E-field scales with $n(z)/n_0$ and the length scales with $n_0/n(z)$, where n_0 is the density at sea level and $n(z)$ is the density at altitude z.

	Total potential		
E-field (STP air)	100 MV	200 MV	400 MV
3.0×10^6V/m ($\sim 10\times E_t$)	$N_{RE}=2.5\times10^5$ $L=33$ m	$N_{RE}=6.0\times10^{10}$ $L=67$ m	4.0×10^{21} $L=133$ m
1.5×10^6V/m ($\sim 5\times E_t$)	$N_{RE}=7.1\times10^4$ $L=67$ m	5.0×10^9 $L=133$ m	$N_{RE}=2.6\times10^{19}$ $L=267$ m
0.7×10^6V/m ($\sim 2.5\times E_t$)	$N_{RE}=4.0\times10^3$ $L=143$m	$N_{RE}=1.6\times10^7$ $L=285$ m	$N_{RE}=2.6\times10^{14}$ $L=571$ m

4.3 Thunderstorms

Thunderstorms are complicated and the picture presented in this section is simplified to only include typically properties of thunderstorms. For more details I refer to the books by *Rakov and Uman* [2003] and *MacGorman and Rust* [1998].

Two hundred and fifty years ago Benjamin Franklin found that thunderclouds are electrically charged, and nearly 100 years ago C.T.R Wilson used ground based measurements to suggest that thunderclouds have a dipole structure with typically positive charge above the negative [*MacGorman and Rust*, 1998, p. 49]. This type of dipole is refereed to as a positive dipole. More recent in-situ measurements of thunderclouds shows that a simple description of a thundercloud can be a positive dipole with a small positive charge region below the main negative [*Rakov and Uman*, 2003, p. 68]. This structure is refereed to as the tripole structure as shown in figure 4.2. The altitudes and charge magnitudes are typically values and are adapted from [*Rakov and Uman*, 2003, p.69].

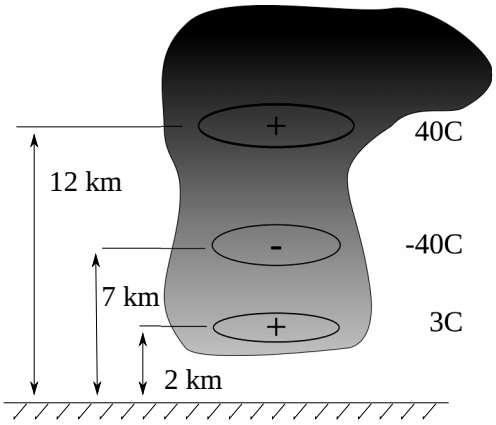

Figure 4.2: The tripole structure of a thundercloud. The altitudes and the magnitudes of the main charge regions are adapted from [*Rakov and Uman*, 2003, p.69]

As the thundercloud charges, via up-draft air, and form the tripole structure, an ambient electric field is build up between the charge regions. Several sounding balloon study have tried to measure the strength of the electrical fields inside thunderclouds. Typical values are higher than the RREA threshold but $\sim 2-3$ times lower than the threshold for conventional breakdown [*Williams*, 2006]. These observations have lead to the suggestion that RREA processes are involved in the initiation of lightning [*Gurevich and Zybin*, 2005; *Dwyer*, 2005], but one cannot reject the hypothesis that local electric field can be much higher and initiates the lightning. As soon as an leader is initiated, the electric field strength needed for leaders to propagate is lower than the conventional breakdown threshold as shown in figure 4.1.

The potential between the main positive and negative charge region is estimated to be $\sim 50-500$ MV [*Rakov and Uman*, 2003, p.111]. However, the highest in-situ measurement of the thundercloud potential is ~ 100 MV [*Marshall and Stolzenburg*, 2001]. Even if there is theoretical suggestion for higher potential in thunderclouds it is likely to assume that ~ 100 MV is a typically maximum potential. With potential above 50 MV the electric field can accelerate electrons up to 50 MeV, which is consistent with the highest photon energies measured in TGFs.

4.3.1 Lightning flash

The lightning flash is the entire process including leader formation, the stage where the leader connects two charge regions, either inside the clouds or from cloud to ground, and finally the discharge of the electrical fields via high currents flowing in the leader channels. A globally estimate of the lightning flashes are 44 ± 5 flashes per second [*Christian*, 2003]. They are most frequent in tropical regions over the continents. Figure 4.3 shows a map of the annual lightning flash rate from LIS/ODT. LIS and OTD are optical satellite born instruments which record the optical emissions from the lightning flashes. LIS/OTD cannot distinguish between IC or CG flashes. More information about LIS/OTD can be found in *Christian* [2003].

About 90% of the lightning flashes are intra cloud (IC) lightning between the main charge regions as seen in figure 4.2, and the remaining 10% are cloud to ground (CG) lightning [*Rakov and Uman*, 2003, p.108]. When CG lightning strikes the ground they produce a high current, called the return stroke. IC lightning do not strike any high conducting regions and therefore contain weaker current pulses [*Rakov and Uman*, 2003, p.341]. Due to the high current in the return stroke (high peak current) CG lighting emits more VLF radiation such that VLF networks are biased to locate CG lightning.

4.4 Production mechanisms for TGFs

As discussed above a thundercloud has the potential sufficient to produce photons with energies of several tens of MeV. In addition to the ambient field between the main charge regions, there are other electric fields which are candidates for TGF production. The following sections will discuss the production mechanisms of TGFs.

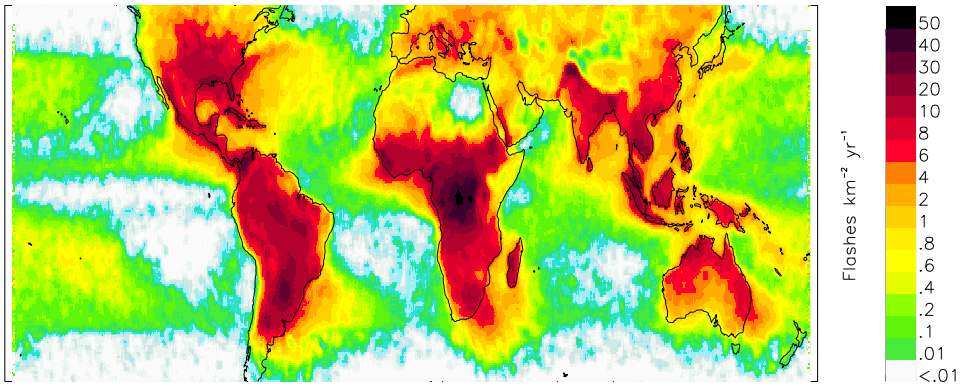

Figure 4.3: The annual lightning flash rate from LIS/ODT. The data are adapted from `http://thunder.nsstc.nasa.gov/data/`.

4.4.1 Quasi electro-static fields

A lightning discharge, either IC or CG, will discharge the electric field on a time scale much shorter than the relaxation time of the screening charges which surrounds the main charge regions. As a result a Quasi electro-static (QS) field will be present above the thunder cloud [*Pasko et al.*, 1995; *Lehtinen et al.*, 1996]. Figure 4.4 shows a simple model of the QS field after an IC lightning with the parameters in figure 4.2. The model assumes that the positive charges (40 C) is distributed uniformly inside a sphere with radius 1 km with located at 12 km altitude. The negative charge region (-40 C) is located at 7 km in a similar sphere. The lower positive region, as shown in figure 4.2, is ignored. An IC lightning stroke between the charge layers is modelled as a fast current which neutralize the charge regions. As a result the screening charges around the charge regions will make an quasi electro static field. The relaxation time for the screening charges are in order of seconds at 12 km altitude and longer at lower altitudes [*Rycroft*, 2000]. If we assume that the lightning discharge is much shorter than the relaxation time a quasi electrostatic field above the initial positive charge region is given by

$$E = \frac{Q}{4\pi\varepsilon_0}\left(\frac{1}{(z-h_t)^2} - \frac{1}{(z-h_m)^2}\right) \ , \ z > h_t + R \tag{4.4}$$

where, Q is the charges of the main charge regions, $\varepsilon_0 = 8.85 \cdot 10^{-12}$ F/m (the electric constant), $h_t = 12$ km, $h_m = 7$ km and $R = 1$ km, which is the radius of the charge sphere. Inside the sphere, with radius R, of positive charge $(12 - 13$ km) the electric field is given by

$$E = \frac{Q}{4\pi\varepsilon_0}\left(\frac{z-h_t}{R^3} - \frac{1}{(z-h_m)^2}\right) \ , \ z \in (h_t, h_t + R]. \tag{4.5}$$

The first terms in equation 4.4 and 4.5 are from the main positive charge region and the last terms are the contribution from the main negative charge region.

Equation 4.4 and 4.5 are plotted in figure 4.4. The dashed line in figure 4.4 is the

electric field threshold for RREA, E_t, and the dotted line is the threshold for conventional breakdown, E_k.

$$E_t = 3.0 \times 10^5 [V/m] \times \exp\{-z/H\} \tag{4.6}$$

$$E_k = 3.2 \times 10^6 [V/m] \times \exp\{-z/H\} \tag{4.7}$$

where H is the atmospheric scale hight of 7 km.

This simple model of an IC lightning shows that one may exceed the conventional threshold at $\sim$ 90 km altitude and the RREA threshold at $\sim$ 70 km. But it also shows that the RREA threshold is exceeded very close to or inside the thundercloud. For the case shown in figure 4.4 the total potential when $E > E_t$ in the region 12-15 km is $\sim$ 118 MV.

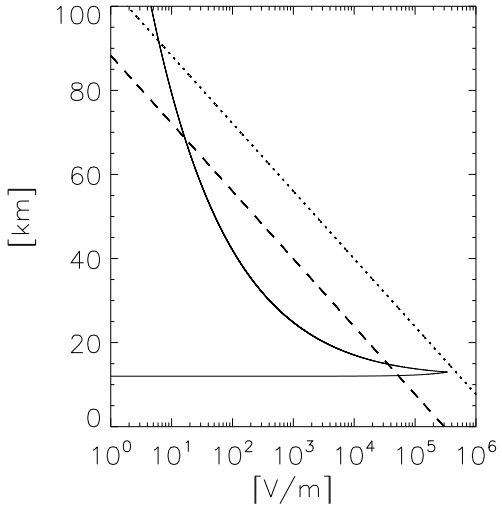

Figure 4.4: A simplified model of the electric field, E, after an intra cloud lightning is shown in solid. The threshold for RREA, E_t ,is dashed and the threshold for conventional breakdown, E_k, is dotted.

Lehtinen et al. [1997] simulated runaway avalanches in QS fields and found that they could produce TGFs at heights of 60-70 km. Their simulations result were comparable to those measured by BATSE if the lightning brought > 250 C from cloud to ground. In a later study *Lehtinen et al.* [1999] found that if the geomagnetic field was included in the simulations the QS field could only produce TGFs below $\sim$ 40 km altitude. At altitudes > 40 km the electrons gyro frequency around magnetic field lines are larger than the collision frequency such that one cannot accelerate the electrons in the electric field direction and gain the required energy for runaway avalanches. To produce the photon fluxes measured at satellite altitudes the theoretical models for QS needed extremely high charge moment change ($\sim$ 2500 Ckm) from the lightning making the QS field [*Lehtinen et al.*, 2001]. This indicates that TGFs produced by QS fields should be a rare phenomena, which was consistent with the low BATSE detection rate (78 TGFs in eight years), but not with the more recent observation by RHESSI, Fermi

and AGILE. Also, the mean charge moment change found in lightning associated with TGFs by the *Cummer et al.* [2005] is 49 Ckm which is far less than the ($\sim$ 2500 Ckm) needed in the QS model. *Gurevich et al.* [2004] suggested that QS fields inside a thundercloud at $<$ 20 km altitude could produce TGFs. But due to atmospheric attenuation this theory also needs very large charge moment to make enough initial photons in a TGFs that are detectable at satellite altitude. However, *Gurevich et al.* [2004] did not include feedback effects in this estimate. How feedback would change their results are not studied.

4.4.2 TGF produced by an electromagnetic pulse

The TGF observations by RHESSI reported 10-20 TGFs per month [*Smith et al.*, 2005]. The increased number of observed TGFs could not be explained by the QS-field model and therefore *Inan and Lehtinen* [2005] suggested that TGFs could be produced in the electrical fields from an electromagnetic pulse (EMP) emitted by the lightning return stroke. However, their model implies very high peak currents with peak currents ($>$ $450-700$ kA) and fast return strokes (99-99.5% the speed of light). Such lightnings are rare and they concluded that EMP fields could produce $\sim 6-8$ TGFs per day which is less than the estimate of $\sim$ 50 TGFs per day by *Smith et al.* [2005] and far less than more recent estimates like 220-250 TGFs per day [*Fuschino et al.*, 2011] and $>$ 50.000 TGFs per day [*Østgaard et al.*, 2012].

4.4.3 The relativistic feedback discharge model

The relativistic feedback discharge model of (RFD) terrestrial gamma ray flashes is developed by Dwyer in numerous papers [*Dwyer*, 2003, 2007, 2012]. As shown in table 4.2 the avalanche growth factor in electric field varying from $\sim 2.5-10$ times E_t provides fewer electrons than the $10^{16}-10^{18}$ required in an average RHESSI TGF. Only if the total potential is in the order of $\sim$ 400 MV and the electrical field is close to the conventional breakdown threshold (E_k) the needed number of electrons by RREA can be obtained. As discussed in section 4.2 such fields are not likely to occur in thunderstorms.

The feedback idea was presented in *Dwyer* [2003] where he modelled RREA involving positive feedback effects from positrons and photons. In this model the runaway electrons produce X- and gamma-rays that may be backscattered via Compton scattering. The downward propagating photons may then create secondary avalanches via Compton scattering and photoelectric absorption. Alternatively, the gamma-photons in a RREA may produce positrons via pair production. Such positrons may turn around and propagate in the opposite direction of the electric field. As a result one would get runaway positrons which create secondary avalanches. Via this positive feedback effects the runaway discharge may become self sustaining leading to a dramatic increase in the number of produced relativistic electrons. Figure 4.5 shows a Monte Carlo simulations from *Dwyer* [2007] where runaway electrons trajectories are black and positrons are blue. The top panel contain particles at time $t < 0.5$ μs ,the middle at $t < 2$ μs and bottom at $t < 10$ μs. The figure shows how rapidly the RFD model increases the number of runaway electrons and leads to a breakdown of the electric field.

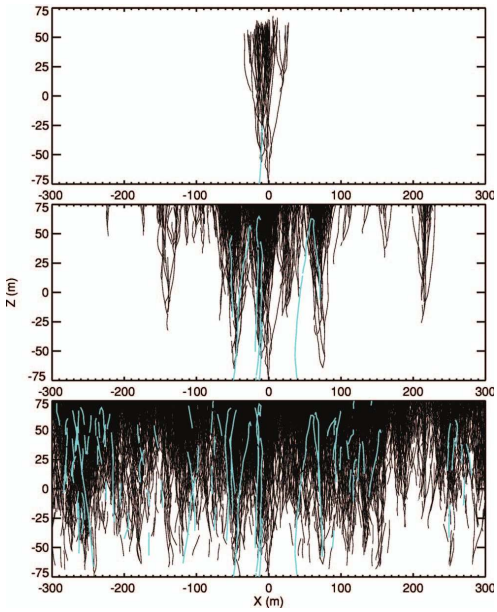

Figure 4.5: RFD in a 750 kV/m electric field at STP air. Black trajectory are runaway electrons and blue are positrons traveling back and creating new avalanches. Top panel is for time $t < 0.5$ μs , middle $t < 2$ μs and bottom $t < 10$ μs. The figure is from *Dwyer* [2007].

The feedback factor, γ_D, is defined as the number of runaway electrons in an avalanched divided by the number of runaway electrons in the previous avalanche. If $\gamma_D = 1$ the avalanche will be self-sustaining. If $\gamma_D > 1$ the number of runaway electrons will grow with time, and discharge the electric field.

In order for RFD to be efficient in the production of TGF high potential is needed [*Carlson et al.*, 2009]. The potential used in RFD are typically 200-400 MV, but *Dwyer* [2012] have found that RFD can generate a TGF in potential as low as 50 MV if the average electric field is near the conventional breakdown field. This would correspond to an electric field of $\sim 3 \times 10^6$ V/m over a region of < 20 m in STP air and $\sim 1 \times 10^6$ over < 60 m at 8 km altitude.

The RFD model of TGFs suggests that the runaway electrons in a TGF produce large currents. *Dwyer* [2012] estimated this current to be comparable to or larger than the currents produced in IC lightnings and consequently emits sferic of VLF-frequency. *Dwyer* [2012] further suggests that ground based lightning detection network such as WWLLN misidentifies the sferic from TGFs as lightning discharges. This could explain the close connection which has been found between TGF and sferics [*Connaughton et al.*, 2010; *Cohen et al.*, 2010b; *Collier et al.*, 2011]. Also, a new type of sferic related to TGFs are recently discovered. *Cummer et al.* [2011] found a strong temporal connection between the Fermi gamma-ray count rate and a slower process sferics data. This slow process could be the signature expected from the TGF producing electron avalanche [*Dwyer*, 2012].

4.4.4 Cold relativistic runaway electron avalanches

Cold RREA suggest that thermal electrons are accelerated over the peak of the friction force, which is shown in figure 4.1. This means that the electric field locally has to be above ~ 280 kV/cm. A significant work by *Moss et al.* [2006] show that it is possible for electrons to become runaway in the strong fields around streamer and leader tips. They're simulations show that the electric field in the streamer tip may be $\sim 10E_k$, which is the field needed to push the thermal electrons over the peak in the friction force and into the runaway regime. Production of thermal runaway electrons in streamers and leaders are also found in other theoretical studies e.g *Chanrion and Neubert* [2008, 2010].

In a leader step *Moss et al.* [2006] estimate the runaway electron production rate to 10^{18} s^{-1} which is $\sim 10^{12}$ for a 1 μs leader step. In a survey of relevant lightning physics *Carlson et al.* [2009] suggests that TGFs are produced in a current pulse. In this mechanism a current pulse would create cold runaway electrons that are seeded in the strong electric field close to the leader tip or leader channel and undergo RREA. Due to the high number of seed electrons $\sim 10^{12}$ only 'small' ($\sim 10^4 - 10^6$) avalanche multiplication is needed to make a TGF observable in space.

Further investigations of cold runaway is done by *Celestin and Pasko* [2011]. They have found that it is possible to gain $\sim 10^{17}$ energetic electrons in a corona streamer flash from a negative leader such that no further avalanche multiplication is needed. The duration of a corona flash is short (~ 10 μs). Therefore *Celestin and Pasko* [2012] suggest that Compton dispersion of photons, as described in *Østgaard et al.* [2008], will make the event ~ 50 μs when observed at satellite altitudes. A TGF duration of 50 μs is consistent with the new results from Fermi [*Fishman et al.*, 2011]. The longer events,

such as the estimate from *Gjesteland et al.* [2010] which found that the BATSE TGF was ~ 250 μs at origin, are explained by *Celestin and Pasko* [2012] as overlapping emissions from individual leader steps. In each leader step a TGF is emitted, and if the time between the leader steps is small the dispersion by Compton scattering would combine the individual events into one TGF at satellite altitude.

4.5 Summary of TGF production theories

When TGFs were first discovered they're origin were placed at > 40 km altitude [*Nemiroff et al.*, 1997] and they were though to be related to read sprites. Also, because the high attenuation of gamma in the atmosphere *Nemiroff et al.* [1997] argued that altitudes above 40 km are the most likely source for TGFs. As a consequence Wilson's original idea about the QS field above thunderclouds was suggested to produced TGFs. However, due to the influence of the geomagnetic field, it was shown that the QS-model could not produce TGFs above ~ 40 km altitude [*Gurevich et al.*, 2004; *Lehtinen et al.*, 1999]. The idea that TGFs were produced in a QS field below 40 km altitude was rejected since the model needed extremely high charge moment changes to make a TGF detectable in space [*Lehtinen et al.*, 2001]. The idea that TGFs were produced in the electric field from an EMP can explain TGF produced at altitudes > 40 km, but this idea also require strong lightning discharges and it can only account for some of the TGF observations [*Inan and Lehtinen*, 2005].

The spectral analysis of TGFs [*Dwyer*, 2005; *Carlson et al.*, 2007; *Østgaard et al.*, 2008; *Gjesteland et al.*, 2010] all suggest that TGFs are produced below ~ 20 km altitude. These results are also an argument against the QS model at high altitude and the EMP model.

As shown in section 4.2 the avalanche multiplication factor are too low to produce TGFs. It is therefore suggested that cosmic ray secondary particles could act as seed particles to increase this number to the required $10^{16} - 10^{18}$ electrons. The number of relativistic seed particles from cosmic rays are typically $\sim 10^6$ per TGF [*Carlson et al.*, 2008]. However, this number may increase significantly if a very high energy cosmic ray deposit its energy at the right place at the right time. But such cosmic rays are too rear to account for the number of TGFs detected so far [*Carlson et al.*, 2008]. *Dwyer* [2008] Also concludes that an external sources of seed particles, such as cosmic rays, are insufficient to account for TGF fluxes.

Today there the most compelling theories are that TGFs are either produced via cold RREA or by the RFD model of TGF. The RFD model assumes that the TGFs are emitted as the lightning leaders develops between the main charge regions of the thunder cloud [*Dwyer*, 2012]. This implies that the TGF should occur before the lightning. If very accurate VLF data are available it may be possible to test whether TGFs do occur before the lightning. However, *Dwyer* [2012] suggests that the RREA itself produce a sferic which is observable in VLF radio and that VLF detectors will misinterpreter this pulse emitted by RREA as the lightning. *Dwyer* [2012] suggests that the slow radio pulse measured by *Cummer et al.* [2011] is evidence for the latter.

RFD can also explain the multi pulse TGFs, which is common in the BATSE measurements, but not in RHESSI. The main problem with RFD is the required potential needed to make feedback important. *Dwyer* [2012] shows that typically values are 200-

400 MV which is less than the measured values in thunderstorms ($\sim$ 100 MV [*Marshall and Stolzenburg*, 2001]). It is, however, still not known what the maximum potential in thunderstorms is [*Dwyer*, 2012].

In the new search of the RHESSI data *Gjesteland et al.* [2012] found more than twice as many TGFs as previously reported. *Østgaard et al.* [2012] studied the relative detection rates between RHESSI and Fermi and argue that one cannot reject the hypothesis that all lightning produce TGFs. These studies indicates that TGFs are a common phenomenon and therefore may be produced in thunderstorms with lower potentials than needed in the RFD model. More studies of potentials in thunder clouds are needed to address this question.

In the RFD model *Dwyer* [2012] assumes that the TGFs are produced in the ambient field between the main charge regions of the thundercloud. As shown in section 4.4.1, with the simplified model of a QS-field, it is also possible for RFD to be efficient in the QS field of a modest IC lightning. When *Lehtinen et al.* [2001] rejected the QS model at < 40 km altitude, they did not include feedback effects. Whether or not their conclusions would change if they included feedback effects should be investigated further. If RFD occur in a QS field one would expect the TGFs to be emitted towards the end of, or after the lightning discharge.

Experiments have found X-rays in laboratory sparks. Both *Rahman et al.* [2008] and *Nguyen et al.* [2008] have used a 1 MV Marx generator to produce $\sim$ 1 m long sparks in STP air. Both studies reports of X-ray emission together with the spark. It is also found that lightning leader steps emits gamma-rays. *Moore et al.* [2001] found burst of gamma radiation before three negative lightning strokes. They suggest that the gamma emission were associated with the leader step. With a collimated gamma-detector *Dwyer et al.* [2011] measured gamma photons emitted from the tip of the lightning leader as it propagates down towards the ground. These observations, together with the results from laboratory sparks are manifestations that cold runaway electrons are produced in leaders and streamers. The question is whether or not cold runaway acceleration are effective enough to make the amount of photons and the high photon energies that is measured in a TGF.

The width of the initial photon emission in a TGF is suggested to be $30^\circ - 40^\circ$ [*Gjesteland et al.*, 2011]. This is also consistent with the results from *Carlson et al.* [2007] and *Hazelton et al.* [2009]. Such emission implies that the electric field is vertical or nearly vertical ($< 20^\circ$ from vertical) orientated electric field. Both RFD and the simulation from *Celestin and Pasko* [2012], where TGF are suggested to be produced in the electrical field from leaders, implies comparable spatially broadening of the gamma emissions.

One can not reject the hypothesis that both RFD and cold runaway accelerations are involved in the production of TGFs. In the RFD model it is assumed that the TGFs occurs while the lightning leaders develops. It would be interesting to investigate how the RFD model is modified when cold runaway seeding are included, and whether seeding from streamers and leaders are more important than the increase in the avalanche growth factor due to feedback.

4.6 Terrestrial Electron Beams

Lehtinen et al. [2000, 2001] found that the runaway electrons that produces TGF, and the knock off electrons from Compton scattering, could escape the atmosphere. Such electrons will be bounded to the geomagnetic field and escape the Earth's atmosphere as a beam. Figure 4.6 shows a possible TGF electron beam first found by *Smith et al.* [2006]. This event occurred event on January 17, 2004 when RHESSI was over the Sahara dessert, which is not a place where one expects to find lightning activity. They suggest that this was an electron beam coming from the conjugate hemisphere. As shown in figure 4.6 the lightcurve shows two pulses. The first pulse is the direct electron beam coming from the conjugate hemisphere while the second pulse is electrons which have mirrored due to the increase in magnetic field strength and moves upwards again.

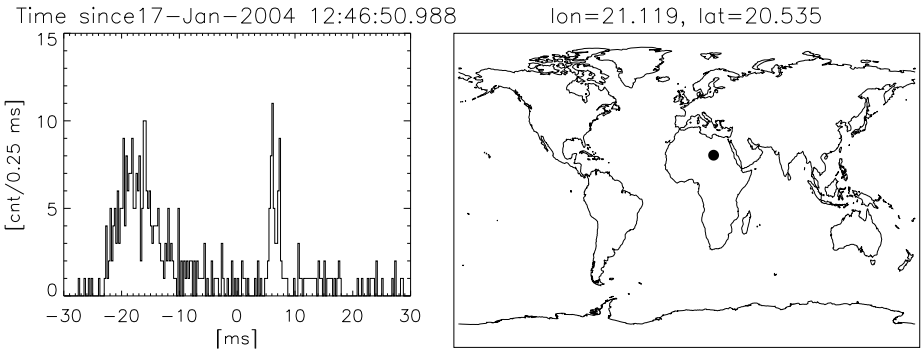

Figure 4.6: The lightcurve of the electron beam on Januar 17 2004. The map shows the RHESSI sub-satellite point a the time of the detection.

Similar events are also found in BATSE. *Dwyer* [2008] suggests that six of the 36 BATSE TGFs they analysed were electron beams. *Briggs et al.* [2011] identified electron beams measured by Fermi GBM. Spectral analysis from these electron beams shows strong 511 keV positron annihilation lines, which indicates that a significant portion (estimated to 11 %) of the particles that escape the atmosphere are positrons created by pair production. The electron beams measured by Fermi GBM were also connected to specific lightning strokes, which were from the most intense part of the distribution (peak current) of their thunderstorms [*Cohen et al.*, 2010c].

Carlson et al. [2011] have simulated electrons beams produced by TGFs and estimated the ratio of detected TGFs per electron beam for satellite borne instruments. This ratio was measured to 5 (30 TGF and 6 electron beams) for BATSE [*Dwyer et al.*, 2008] and 13 (77 TGFs and 6 electron beams) for Fermi [*Briggs et al.*, 2011]. This large fraction of electron beams are most likely biased due to the long trigger windows in BATSE and Fermi. If the ratio is 10 then it implies that the effective observation radius for TGF observation by satellite instrument are $\leq$ 100 km [*Carlson et al.*, 2011, Figure 5], which is not consistent with the geolocation of TGFs, which find TGFs out to $\sim$ 800 km from the sub satellite point [*Cohen et al.*, 2010b; *Collier et al.*, 2011]. In comparing there have, so far, only been identified one electron beam in the RHESSI data [*Smith et al.*, 2006] (Figure 4.6).

Chapter 5

Summary of papers

5.1 Paper I: Production altitude and time delays of the terrestrial gamma flashes: Revisiting the Burst and Transient Source Experiment spectra

The motivation for this paper was, for the first time, to do spectral analysis of individual TGFs. Previously spectral analysis of TGFs had only used superposed spectrum [*Dwyer and Smith*, 2005; *Carlson et al.*, 2007], and the effect of mixing spectra observed at different angles were not known. At this time it was also an open question whether TGFs were produced at high altitude, as the BATSE data indicated [*Fishman et al.*, 1994; *Nemiroff et al.*, 1997], or at lower altitudes as the more recent RHESSI data indicated [*Dwyer and Smith*, 2005; *Cummer et al.*, 2005; *Carlson et al.*, 2007].

A Monte Carlo simulation, which accounted for photoelectric absorption, Compton scattering, pair production and bremsstrahlung from Compton electrons, were developed. The Monte Carlo simulation were tested against the GEANT simulation tool with good agreement. The simulation inputs were different production altitudes and initial distributions of photons spatial and spectral.

Only based on the simulations several features of TGFs were discovered. The energy spectrum has a low energy cut off which moves to lower energies as the production altitude increases. Also the energy spectra of TGFs at large angles has a softer energy spectrum which is a result of Compton scattering. The time dispersion between high and low energy photons as described by *Feng et al.* [2002] are also found in the simulations if the production altitude are below ~ 20 km. This is also explained as an effect of Compton scattering. The high energy photons have a more straight way through the atmosphere than the lower energy photons. Lower energy photons that escape the atmosphere were originally of higher energies, but reduced in energy as they were Compton scattered on their way from the production altitude to the satellite.

By comparing the simulation results to the BATSE measurements the production altitude were determined to be below 20 km. However, a significant portion of the TGFs were found to be produced at higher altitudes e.g. $30-40$ km. These TGFs were single pulse with high fluxes.

It is also found a softening in the BATSE spectra for increasing observation angles. This is also interpreted as an effect of Compton scattering. Assuming a narrow emission of the photons in a TGF, only scattered photons, which are reduced in energy, are

detected at large angles.

5.2 Paper II: Effects of dead-time losses on terrestrial gamma ray flash measurements with the Burst and Transient Source Experiment

Shortly after the analysis of the BATSE data by *Østgaard et al.* [2008] is was shown that BATSE suffered from dead-time saturation [*Grefenstette et al.*, 2008]. By comparing the peak fluxes in BATSE and RHESSI *Grefenstette et al.* [2008] found that BATSE TGFs could have ~ 4 times higher peak fluxes than measured. These findings questioned all results based on the BATSE measurements. Since BATSE operates in a trigger mode, with long trigger window (64 ms) compared to the duration of TGFs, BATSE was biased to multi pulse TGFs. The single pulse TGFs needed very high fluxes to be triggered. Therefore, in order to quantify the effect of the dead-time saturation, five single pulse BATSE TGFs were re-analysed.

Based on pre-flight measurements and documentation *Grefenstette et al.* [2008] showed that BATSE were a paralyzable detector with energy dependent dead-time. In Paper II the properties of the BATSE read-out electronics were implemented in a Monte Carlo model.This Monte Carlo model was used to determine the effects of dead-time in BATSE.

The main result is that the energy spectrum becomes softer for increased losses due to dead-time. In a TGF the high energy photons arrive before the low energy photos due to the Compton dispersion as described in *Østgaard et al.* [2008]. Since the high energy photons arrive earlier, at the time when the flux in the TGFs are the highest, mostly high energy photons are lost due to dead-time. The later arriving Compton tail are not as influenced by the dead-time losses.

When the dead-time corrected simulated spectrum are compared to BATSE measurements it results in a lower estimated production altitude. All the single pluse TGFs with high fluxes are now determined to be produced < 20 km altitude.

Since BATSE was a paralysable detecor it is also found that a double pulse TGF measured by BATSE were in fact a single pulse. But since the dead-time losses increases dramatically for high fluxes this TGF may be measured as a double pulse. If this is the case, this TGF is in fact 6 times brighter than measured.

By only investigating the highest energy channel of BATSE (>300 keV) an estimate of the TGF production time were made. These 5 single pulse TGF are estimated to last between $200 - 555$ μs, which is less than the previously assumed ~ 1 ms duration and consistent with later detailed analyses of Fermi TGFs [*Fishman et al.*, 2011; *Briggs et al.*, 2010].

5.3 Paper III: Confining the Angular Distribution of Terrestrial Gamma-ray Flash Emission

The basic idea in this study is that the initial angular distribution of the TGF emission will reflect the electric fields that produces TGFs.

The 106 TGFs, which were geolocated by AWESOME [*Cohen et al.*, 2010b] and WWLLN [*Collier et al.*, 2011], were available for this study. To compare these measurements to simulations two approaches were used. First the the distribution of observation angles, which is the angle between RHESSI nadir and a straight line to the source lightning, which is assumed to be the location where the TGFs are produced, are compared to a simulation of the expected observation angle distribution. In the simulations assumptions were made about the TGFs energy spectrum, production altitude, spatially distribution and intensity distribution. The energy spectrum were assumed to be a RREA spectrum ($dn/d\varepsilon \propto 1/\varepsilon$). The production altitude were from 15-20 km and the spatially distribution were assumed to be isotropical within a cone with half angle ranging from $10^\circ - 60^\circ$. The initial number of photons in each TGF were assumed to be distributed according to a power law, which is shown to be feasible [*Collier et al.*, 2011], with the spectral index ranging from 1.5 to 3. With these assumptions the Monte Carlo simulations from *Østgaard et al.* [2012] were used to simulate the photons through the atmosphere. At satellite altitude all TGFs which have a fluence larger than the detection threshold where included in the simulated observation angle distribution. This distribution is a competition between the area, which is increasing at increasing observation angle, and the TGF fluence, which is decreasing at increasing observation angle.

The simulated observation angle distribution were compared to the observed distribution with a Kolmogorov-Smirnov two-sample test and it shows that simulations where the photons were emitted within a cone with half angle $> 30^\circ$ can represent the measurements.

The dataset contained 10 TGFs which were observed at large angles ($> 40^\circ$). The spectrum from these TGFs were superposed and compared to simulated spectra. The superposed RHESSI spectrum of TGF measured at large angles is significantly softer than the superposed RHESSI spectrum from smaller angles. This is also found in simulations were the emission cone had a half angle $< 40^\circ$.

With the results from the observation angle distribution and the results from the spectral analysis of TGFs measured at large angles *Gjesteland et al.* [2011] confine the TGF emission to a cone with half angle of $30^\circ - 40^\circ$.

If one assumed that the TGF intensities are distributed as a power law the simulations found that the spectral index of the intensity distribution is confined within 1.9 and 2.5.

5.4 Paper IV: A new method reveals more TGFs in the RHESSI data

I has been suggested in the TGF community that the instruments so far has only detected the tip of the iceberg. Meaning that if one increases the sensitivity of ones instrument the number of detected TGFs would increase significantly. For example the increase from the 78 TGFs found in BATSE to the ~ 1000 found by RHESSI is due to a better sensitivity in RHESSI since RHESSI do not work in a trigger mode. Also Fermi GBM increased the number of identified TGFs when the sensitivity threshold was reduced [*Briggs*, 2011].

In the RHESSI catalog paper *Grefenstette et al.* [2009] present results from an additional search algorithm applied on the RHESSI data. The algorithm is not described

and neither is the quality and number of new events quantified. But it clearly indicates that there are more TGFs in the RHESSI data than presented in the RHESSI catalog. This was the motivation to develop a new search algorithm and apply it on the raw RHESSI data. The new search algorithm were based on Poison statistic with search windows 0.3 ms, 1 ms and 3 ms. Also the possible events had to pass five selection criteria which were based on properties of TGFs from the RHESSI catalog and other measurements.

In the RHESSI data from 2004, 2005 and 2006 the new algorithm identified 1012 TGFs. This is more than twice as many as in the RHESSI catalog, which presented 474 for the same period. The new TGFs follows the same seasonal and geographical variation as previously identified TGFs, and they also follow the seasonal pattern of lightning activity.

The new RHESSI TGFs have also been matched with WWLLN sferics by the method as presented in *Collier et al.* [2011]. Of the 1012 new TGFs 91 were matched with WWLLN events. This is comparable with the results presented in *Collier et al.* [2011].

5.5 Paper V: The true fluence distribution of terrestrial gamma flashes at satellite altitude

Since *Gjesteland et al.* [2012] found more than twice as many TGFs by relaxing the search algorithm, this study's motivation was to determine how big the 'iceberg' of TGFs actually is. It is important to know how common TGFs are in order to put constrains on the production mechanism.

If one assume that the fluence distribution of TGFs follows a power law as suggested by *Collier et al.* [2011], one expects that RHESSI and Fermi GBM are mesuring TGFs from the same distribution. However, the two instruments have different orbits, effective area and sensitivity threshold. If these differences are corrected for one can compare the daily TGF detection rate to obtain the true fluence distribution. By this method *Østgaard et al.* [2012] show that the TGF fluence distribution follows a power law with spectral index 2.3 ± 0.2 at satellite altitudes.

It is known that RHESSI suffers from losses due to dead-time [*Grefenstette et al.*, 2008] (se section 3.6). The losses due to dead-time are most significant for the events with highest fluxes. As a consequence the weak TGF are hardly influenced by dead-time losses, while the stronger ones are. If one fits a power law curve to the measured fluence distribution of RHESSI, one get a spectral index of 3.5, which is larger than the 2.3 mentioned above. Therefore a simulation to calculate the losses due to dead-time were applied on the RHESSI measurements. This method clearly shows that the TGFs with highest fluence suffer more from dead-time losses than the TGFs with lower fluence. A power law fit to the dead-time corrected RHESSI fluence distribution is found to have a spectral index between 2.3 and 3.0. The dead-time corrected RHESSI fluence distribution also shows indications of a roll off with a spectral index of 1.7 for the lower part of the distribution.

The fluence distribution at the source are found to be different than the measured fluence distribution at satellite altitude. If one uses the method from *Carlson et al.*

[2012] one find that the spectral index for the distribution at the production altitude is shifted to lower spectral indexes. E.g. if the true fluence distribution in space have a spectral index 2.3 ± 0.2, which the results in *Østgaard et al.* [2012] indicates, than the fluence distribution at the production altitude have a spectral index 2.0 ± 0.2.

If one assume a sharp cut-off at 5/600 of the RHESSI sensitivity threshold and that the true TGF fluence distribution of TGFs follows a power law with spectral index 2.0 the estimated number of TGFs within $\pm 38^\circ$ latitude are 50.000 TGFs/day, which is $\sim 2\%$ of all IC lightning. If one assumes a roll off with spectral index 1.7 at satellite altitudes which corresponds to 1.3 at the source one cannot reject the hypothesis that all lightning produces TGF. Both the scenarios above are consistent with the results from ADELE, which only detected one TGF even if the detector was within 10 km of 1213 lightning flashes [*Smith et al.*, 2011].

The results are also consistent with *Gjesteland et al.* [2012] who identified more than twice as many TGFs by reducing the lower detection threshold from ~ 17 counts per TGF, as used by *Grefenstette et al.* [2009], to ~ 12 counts per TGFs, which are the weakest TGFs found in the new search by *Gjesteland et al.* [2012].

This paper also shows that the dead-time losses in an average RHESSI TGF is $\sim 25\%$.

Bibliography

Abarca, S. F., K. L. Corbosiero, and T. J. jr. Galarneau (2010), An evaluation of the Worldwide Lightning Location Network (WWLLN) using the National Lightning Detection Network (NLDN) as ground truth, *Journal of Geophysical Research*, *115*, doi:10.1029/2009JD013411. 3.5

Briggs, M. S. (2011), More TGFs from GBM, in *paper presented at Terrestrial Gamma-Ray Flash Workshop 2011, Cent. for Space Plasma and Aeron. Res., Univ. of Ala., Huntsville.* 3.3, 5.4

Briggs, M. S., et al. (2010), First results on terrestrial gamma ray flashes from the Fermi Gamma-ray Burst Monitor, *Journal of Geophysical Research*, *115*(A7), doi: 10.1029/2009JA015242. 3.3, 3.3, 5.2

Briggs, M. S., et al. (2011), Electron-positron beams from terrestrial lightning observed with Fermi GBM, *Geophysical Research Letters*, *38*(2), doi:10.1029/ 2010GL046259. 4.6

Carlson, B. E., N. G. Lehtinen, and U. S. Inan (2007), Constraints on terrestrial gamma ray flash production from satellite observation, *Geophysical Research Letters*, *34*(8), doi:10.1029/2006GL029229. 3.1, 3.2, 4.5, 5.1

Carlson, B. E., N. G. Lehtinen, and U. S. Inan (2008), Runaway relativistic electron avalanche seeding in the Earth's atmosphere, *Journal of Geophysical Research*, *113*(A10307), doi:10.1029/2008JA013210. 2.3, 4.5

Carlson, B. E., N. G. Lehtinen, and U. S. Inan (2009), Terrestrial gamma ray flash production by lightning current pulses, *Journal of Geophysical Research*, *114*, A00E08, doi:10.1029/2009JA014531. 4.4.3, 4.4.4

Carlson, B. E., T. Gjesteland, and N. Østgaard (2011), Terrestrial gamma-ray flash electron beam geometry, fluence, and detection frequency, *Journal of Geophysical Research*, *116*(A11), doi:10.1029/2011JA016812. 4.6

Carlson, B. E., T. Gjesteland, and N. Østgaard (2012), Connecting the terrestrial gamma-ray flash source strength and observed fluence distributions, *Journal of Geophysical Research*, *117*(A1), doi:10.1029/2011JA017122. 5.5

Celestin, S., and V. P. Pasko (2011), Energy and fluxes of thermal runaway electrons produced by exponential growth of streamers during the stepping of lightning leaders and in transient luminous events, *Journal of Geophysical Research*, *116*(A3), doi: 10.1029/2010JA016260. 4.4.4

Celestin, S., and V. P. Pasko (2012), Compton scattering effects on the duration of terrestrial gamma-ray flashes, *Geophysical Research Letters*, *39*(2), doi:10.1029/2011GL050342. 4.4.4, 4.5

Chanrion, O., and T. Neubert (2008), A PIC-MCC code for simulation of streamer propagation in air, *Journal of Computational Physics*, *227*(15), 7222–7245, doi:10.1016/j.jcp.2008.04.016. 4.4.4

Chanrion, O., and T. Neubert (2010), Production of runaway electrons by negative streamer discharges, *Journal of Geophysical Research*, *115*, doi:10.1029/2009JA014774. 4.4.4

Christian, H. J. (2003), Global frequency and distribution of lightning as observed from space by the Optical Transient Detector, *Journal of Geophysical Research*, *108*(D1), doi:10.1029/2002JD002347. 3.2, 4.3.1

Cohen, M., U. Inan, and E. Paschal (2010a), Sensitive Broadband ELF/VLF Radio Reception With the AWESOME Instrument, *IEEE Transactions on Geoscience and Remote Sensing*, *48*(1), doi:10.1109/TGRS.2009.2028334. 3.5

Cohen, M. B., U. S. Inan, and G. Fishman (2006), Terrestrial gamma ray flashes observed aboard the Compton Gamma Ray Observatory/Burst and Transient Source Experiment and ELF/VLF radio atmospherics, *Journal of Geophysical Research*, *111*(D24), doi:10.1029/2005JD006987. 3.5

Cohen, M. B., U. S. Inan, R. K. Said, and T. Gjestland (2010b), Geolocation of terrestrial gamma-ray flash source lightning, *Geophysical Research Letters*, *37*(2), doi:10.1029/2009GL041753. 3.5, 3.5, 4.4.3, 4.6, 5.3

Cohen, M. B., U. S. Inan, R. K. Said, M. S. Briggs, G. J. Fishman, V. Connaughton, and S. A. Cummer (2010c), A lightning discharge producing a beam of relativistic electrons into space, *Geophysical Research Letters*, *37*(L18806), doi:10.1029/2010GL044481. 4.6

Coleman, L. M., and J. R. Dwyer (2006), Propagation speed of runaway electron avalanches, *Geophysical Research Letters*, *33*(11), doi:10.1029/2006GL025863. 4.2

Collier, A. B., T. Gjesteland, and N. Østgaard (2011), Assessing the power law distribution of TGFs, *Journal of Geophysical Research*, *116*(A10), doi:10.1029/2011JA016612. (document), 3.5, 3.5, 3.8, 4.4.3, 4.6, 5.3, 5.4, 5.5

Connaughton, V., et al. (2010), Associations between Fermi Gamma-ray Burst Monitor terrestrial gamma ray flashes and sferics from the World Wide Lightning Location Network, *Journal of Geophysical Research*, *115*(A12), doi:10.1029/2010JA015681. 3.3, 3.5, 4.4.3

Cummer, S. A., Y. Zhai, W. Hu, D. M. Smith, L. I. Lopez, and M. A. Stanley (2005), Measurements and implications of the relationship between lightning and terrestrial gamma ray flashes, *Geophysical Research Letters*, *32*(8), doi:10.1029/2005GL022778. 3.2, 3.5, 3.5, 4.4.1, 5.1

Cummer, S. A., G. Lu, M. S. Briggs, V. Connaughton, S. Xiong, G. J. Fishman, and J. R. Dwyer (2011), The lightning-TGF relationship on microsecond timescales, *Geophysical Research Letters*, *38*(14), doi:10.1029/2011GL048099. 3.5, 4.4.3, 4.5

Dwyer, J. R. (2003), A fundamental limit on electric fields in air, *Geophysical Research Letters*, *30*(20), doi:10.1029/2003GL017781. 4.2, 4.4.3

Dwyer, J. R. (2005), The initiation of lightning by runaway air breakdown, *Geophysical Research Letters*, *32*(20), doi:10.1029/2005GL023975. 3.1, 4.3, 4.5

Dwyer, J. R. (2007), Relativistic breakdown in planetary atmospheres, *Physics of Plasmas*, *14*(4), doi:10.1063/1.2709652. (document), 4.2, 4.4.3, 4.5

Dwyer, J. R. (2008), Source mechanisms of terrestrial gamma-ray flashes, *Journal of Geophysical Research*, *113*(D10), doi:10.1029/2007JD009248. 3.1, 4.5, 4.6

Dwyer, J. R. (2012), The relativistic feedback discharge model of terrestrial gamma ray flashes, *Journal of Geophysical Research*, *117*(A2), doi:10.1029/2011JA017160. 3.5, 4.2, 4.4.3, 4.4.3, 4.5

Dwyer, J. R., and D. M. Smith (2005), A comparison between Monte Carlo simulations of runaway breakdown and terrestrial gamma-ray flash observations, *Geophysical Research Letters*, *32*(22), doi:10.1029/2005GL023848. 3.2, 4, 5.1

Dwyer, J. R., B. W. Grefenstette, and D. M. Smith (2008), High-energy electron beams launched into space by thunderstorms, *Geophysical Research Letters*, *35*(2), doi:10.1029/2007GL032430. 4.6

Dwyer, J. R., M. Schaal, H. K. Rassoul, M. a. Uman, D. M. Jordan, and D. Hill (2011), High-speed X-ray images of triggered lightning dart leaders, *Journal of Geophysical Research*, *116*(D20), doi:10.1029/2011JD015973. 4.5

Eack, K. B., W. H. Beasley, W. D. Rust, T. C. Marshall, M. Stolzenburg, and M. C. S. Norman (1996), Initial results from simultaneous observation of X rays and electric fields in a thunderstorm, *Journal of Geophysical Research*, *101*(D23), 637–640. 2.3

Feng, H., T. P. Li, M. Wu, M. Zha, and Q. Q. Zhu (2002), Temporal and spectral properties of gamma-ray flashes, *Geophysical Research Letters*, *29*(3), doi:10.1029/2001GL013992. 3.1, 5.1

Fishman, G. J., et al. (1994), Discovery of Intense Gamma-Ray Flashes of Atmospheric Origin, *Science*, *264*(5163), 1313–1316. 1, 2.2, 2.3, 3.1, 3.1, 3.5, 5.1

Fishman, G. J., et al. (2011), Temporal properties of the terrestrial gamma-ray flashes from the Gamma-Ray Burst Monitor on the Fermi Observatory, *Journal of Geophysical Research*, *116*(A7), doi:10.1029/2010JA016084. 2.3, 3.3, 4.4.4, 5.2

Fuschino, F., et al. (2011), High spatial resolution correlation of AGILE TGFs and global lightning activity above the equatorial belt, *Geophysical Research Letters*, *38*(14), doi:10.1029/2011GL047817. 3.4, 4.4.2

Gjesteland, T., N. Østgaard, P. H. Connell, J. Stadsnes, and G. J. Fishman (2010), Effects of dead time losses on terrestrial gamma ray flash measurements with the Burst and Transient Source Experiment, *Journal of Geophysical Research*, *115*, doi: 10.1029/2009JA014578. 1, 3.1, 3.1.1, 3.2.1, 4.4.4, 4.5

Gjesteland, T., N. Østgaard, A. B. Collier, B. E. Carlson, M. B. Cohen, and N. G. Lehtinen (2011), Confining the Angular Distribution of Terrestrial Gamma-ray Flash Emission., *Journal of Geophysical Research*, *116*, doi:10.1029/2011JA016716. 1, 3.2, 3.5, 3.5, 4.5, 5.3

Gjesteland, T., N. Østgaard, a. B. Collier, B. E. Carlson, C. Eyles, and D. M. Smith (2012), A new method reveals more TGFs in the RHESSI data, *Geophysical Research Letters*, *39*(5), doi:10.1029/2012GL050899. (document), 1, 3.2, 3.4, 3.2, 3.5, 3.5, 4.5, 5.5

Grefenstette, B. W., D. M. Smith, J. R. Dwyer, and G. J. Fishman (2008), Time evolution of terrestrial gamma ray flashes, *Geophysical Research Letters*, *35*(6), doi: 10.1029/2007GL032922. 3.1, 3.1, 3.1.1, 3.1.1, 3.1.1, 3.2.1, 5.2, 5.5

Grefenstette, B. W., D. M. Smith, B. J. Hazelton, and L. I. Lopez (2009), First RHESSI terrestrial gamma ray flash catalog, *Journal of Geophysical Research*, *114*(A2), doi: 10.1029/2008JA013721. (document), 1, 2.3, 3.2, 3.2, 3.4, 3.2.1, 3.5, 5.4, 5.5

Gurevich, A., Y. Medvedev, and K. P. Zybin (2004), Thermal electrons and electric current generated by runaway breakdown effect, *Physics Letters A*, *321*(3), 179–184, doi:10.1016/j.physleta.2003.10.062. 4.4.1, 4.5

Gurevich, A. V., and K. P. Zybin (2005), Runaway Breakdown and the Mysteries of Lightning The observed electric fields in thunder, *Physics Today*, *May*, 37–43. 4.3

Gurevich, A. V., G. M. Milikh, and R. Roussel-Dupré (1992), Runaway electron mechanism of air breakdown and preconditioning during a thunderstorm, *Physics Letters A*, *165*, 463–468, doi:10.1016/0375-9601(92)90348-P. 2.3, 4.2

Gurevich, A. V., J. A. Valdivia, G. M. Milikh, and K. Papadopoulos (1996), Runaway electrons in the atmosphere in the presence of a magnetic field, *Radio Science*, *31*(6), 1541–1554. 2.3

Hazelton, B. J., B. W. Grefenstette, D. M. Smith, J. R. Dwyer, X.-M. Shao, S. a. Cummer, T. Chronis, E. H. Lay, and R. H. Holzworth (2009), Spectral dependence of terrestrial gamma-ray flashes on source distance, *Geophysical Research Letters*, *36*(1), doi:10.1029/2008GL035906. 3.2, 4.5

Inan, U. S., and N. G. Lehtinen (2005), Production of terrestrial gamma-ray flashes by an electromagnetic pulse from a lightning return stroke, *Geophysical Research Letters*, *32*(19), doi:10.1029/2005GL023702. 4.4.2, 4.5

Inan, U. S., S. C. Reising, G. J. Fishman, and J. M. Horack (1996), On the association of terrestrial gamma ray bursts with lightning and implications for sprites, *Geophysical Research Letters*, *23*(9), 1017–1020. 3.5

Inan, U. S., M. B. Cohen, R. K. Said, D. M. Smith, and L. I. Lopez (2006), Terrestrial gamma ray flashes and lightning discharges, *Geophysical Research Letters*, *33*(18), doi:10.1029/2006GL027085. 3.5

Knoll, G. (1989), *Radiation Detection and Measurements*, John Wiley, New York. 3.1.1

Lehtinen, N. G., M. Walt, U. S. Inan, T. F. Bell, and V. P. Pasko (1996), gamma ray emission produced by a relativistic beam of runaway electrons accelerated by quasi electrostatic thundercloud fields, *Geophysical Research Letters*, *23*(19), 2645–2648. 4.4.1

Lehtinen, N. G., T. F. Bell, V. P. Pasko, and U. S. Inan (1997), A two dimensional model of runaway electron beams driven by quasi electrostatic thundercloud fields, *Geophysical Research Letters*, *24*(21), 2639–2642, doi:10.1029/97GL52738. 4.4.1

Lehtinen, N. G., T. F. Bell, and U. S. Inan (1999), Monte Carlo simulation of runaway MeV electron breakdown with application to red sprites and terrestrial gamma ray flashes, *Journal of Geophysical Research*, *104*(A11), 24,699–24,712, doi:10.1029/1999JA900335. 4.4.1, 4.5

Lehtinen, N. G., U. S. Inan, and T. F. Bell (2000), Trapped energetic electron curtains produced by thunderstorm driven relativistic runaway electrons, *Geophysical Research Letters*, *27*(8), 1095–1098. 4.6

Lehtinen, N. G., U. S. Inan, and T. F. Bell (2001), Effects of thunderstorm driven runaway electrons in the conjugate hemisphere: Purple sprites, ionization enhancements, and gamma rays, *Journal of Geophysical Research*, *106*(A12), 28,841–28,856, doi:10.1029/2000JA000160. 4.4.1, 4.5, 4.6

Lu, G., et al. (2010), Lightning mapping observation of a terrestrial gamma-ray flash, *Geophysical Research Letters*, *37*(11), doi:10.1029/2010GL043494. 3.5

Lu, G., S. A. Cummer, J. Li, F. Han, D. M. Smith, and B. W. Grefenstette (2011), Characteristics of broadband lightning emissions associated with terrestrial gamma ray flashes, *Journal of Geophysical Research*, *116*(A3), doi:10.1029/2010JA016141. 3.5

MacGorman, D. R., and W. D. Rust (1998), *The electrical nature of storms*, Oxford University Press. 4.3

Marisaldi, M., et al. (2010a), Detection of terrestrial gamma ray flashes up to 40 MeV by the AGILE satellite, *Journal of Geophysical Research*, *115*, doi:10.1029/2009JA014502. 1, 2.3, 3.4, 4

Marisaldi, M., et al. (2010b), Gamma-Ray Localization of Terrestrial Gamma-Ray Flashes, *Physical Review Letters*, *105*(12), doi:10.1103/PhysRevLett.105.128501. 3.4

Marshall, T. C., and M. Stolzenburg (2001), Voltages inside and just above thunderstorms, *Journal of Geophysical Research*, *106*(D5), 4757–4768, doi:10.1029/2000JD900640. 4.2, 4.3, 4.5

Mccarthy, M., and G. K. Parks (1985), Further observations of X-rays inside Thunderstorms, *Physics*, *12*(6), 393–396. 2.3, 4.2

Moore, C. B., K. B. Eack, G. D. Aulich, and W. Rison (2001), Energetic radiation associated with lightning stepped-leaders, *Geophysical Research Letters*, *28*(11), 2141–2144. 4.5

Moss, G. D., V. P. Pasko, N. Liu, and G. Veronis (2006), Monte Carlo model for analysis of thermal runaway electrons in streamer tips in transient luminous events and streamer zones of lightning leaders, *Journal of Geophysical Research*, *111*(A2), doi: 10.1029/2005JA011350. (document), 4.1, 4.4.4

Nemiroff, R. J., J. T. Bonnell, and J. P. Norris (1997), Temporal and spectral characteristics of terrestrial gamma flashes, *Journal of Geophysical Research*, *102*(A5), 9659–9665. 3.1, 3.1, 4.5, 5.1

Nguyen, C. V., a. P. J. van Deursen, and U. Ebert (2008), Multiple x-ray bursts from long discharges in air, *Journal of Physics D: Applied Physics*, *41*(23), doi:10.1088/0022-3727/41/23/234012. 4.5

Østgaard, N., T. Gjesteland, J. Stadsnes, P. H. Connell, and B. Carlson (2008), Production altitude and time delays of the terrestrial gamma flashes: Revisiting the Burst and Transient Source Experiment spectra, *Journal of Geophysical Research*, *113*(A2), doi:10.1029/2007JA012618. 1, 3.1, 3.1.1, 3.2, 4.4.4, 4.5, 5.2

Østgaard, N., T. Gjesteland, R. S. Hansen, a. B. Collier, and B. Carlson (2012), The true fluence distribution of terrestrial gamma flashes at satellite altitude, *Journal of Geophysical Research*, *117*(A3), doi:10.1029/2011JA017365. 1, 3.2.1, 4.4.2, 4.5, 5.3, 5.5

Parks, G. K., B. H. Mauk, R. Spiger, and J. Chin (1981), X-ray enhancements detected during thunderstorm and lightning activities, *Geophysical Research Letters*, *8*(11), 1176–1179. 2.3

Pasko, P., U. S. Inan, Y. N. Taranenko, and F. Bell (1995), Heating, ionization and upward discharges in the mesosphere due to intense quasi-electrostatic thundercloud fields, *Geophysical Research Letters*, *22*(4), 365–368. 4.4.1

Rahman, M., V. Cooray, N. A. Ahmad, J. Nyberg, V. a. Rakov, and S. Sharma (2008), X rays from 80-cm long sparks in air, *Geophysical Research Letters*, *35*(6), doi: 10.1029/2007GL032678. 4.5

Rakov, V. A., and M. A. Uman (2003), *Lightning Physics and Effect*, Cambridge University Press. (document), 3.5, 4.3, 4.2, 4.3, 4.3.1

Rodger, C. J., J. B. Brundell, and R. L. Dowden (2005), Annales Geophysicae Location accuracy of VLF World-Wide Lightning Location (WWLL) network : Post-algorithm upgrade, *Annales Geophysicae*, *23*, 1–14, doi:1432-0576/ag/2005-23-1. 3.5

Roussel-Dupré, R., and A. V. Gurevich (1996), On runaway breakdown and upward propagating discharges, *Journal of Geophysical Research*, *101*(A2), 2297–2311. 2.3

Roussel-Dupré, R. A., A. V. Gurevich, T. Tunnell, and G. M. Milikh (1994), Kinetic theory of runaway air breakdown, *Physical review E*, *49*(3), 2257–2271. 2.3

Rycroft, M. (2000), The global atmospheric electric circuit, solar activity and climate change, *Journal of Atmospheric and Solar-Terrestrial Physics*, *62*(17-18), 1563–1576, doi:10.1016/S1364-6826(00)00112-7. 4.4.1

Shao, X.-M., T. Hamlin, and D. M. Smith (2010), A closer examination of terrestrial gamma-ray flash-related lightning processes, *Journal of Geophysical Research*, *115*(April 2004), doi:10.1029/2009JA014835. 3.5

Smith, D. M., L. I. Lopez, R. P. Lin, and C. P. Barrington-Leigh (2005), Terrestrial gamma-ray flashes observed up to 20 MeV., *Science*, *307*(5712), 1085–8, doi:10.1126/science.1107466. 1, 3.2, 4, 4.4.2

Smith, D. M., et al. (2006), The Anomalous Terrestrial Gamma-ray Flash of 17 January 2004, *EOS Transactions AGU Fall Meeting Supplement*, *87*(52), Abstract AE31A—-1040. 4.6, 4.6

Smith, D. M., B. J. Hazelton, B. W. Grefenstette, J. R. Dwyer, R. H. Holzworth, and E. H. Lay (2010), Terrestrial gamma ray flashes correlated to storm phase and tropopause height, *Journal of Geophysical Research*, *115*, doi:10.1029/2009JA014853. 3.2

Smith, D. M., et al. (2011), The rarity of terrestrial gamma-ray flashes, *Geophysical Research Letters*, *38*(8), doi:10.1029/2011GL046875. 5.5

Splitt, M. E., S. M. Lazarus, D. Barnes, J. R. Dwyer, H. K. Rassoul, D. M. Smith, B. Hazelton, and B. Grefenstette (2010), Thunderstorm characteristics associated with RHESSI identified terrestrial gamma ray flashes, *Journal of Geophysical Research*, *115*, doi:10.1029/2009JA014622. 3.2

Stanley, M. a., X.-M. Shao, D. M. Smith, L. I. Lopez, M. B. Pongratz, J. D. Harlin, M. Stock, and A. Regan (2006), A link between terrestrial gamma-ray flashes and intracloud lightning discharges, *Geophysical Research Letters*, *33*(6), doi:10.1029/2005GL025537. 3.5

Tavani, M., et al. (2011), Terrestrial Gamma-Ray Flashes as Powerful Particle Accelerators, *Physical Review Letters*, *106*(1), doi:10.1103/PhysRevLett.106.018501. 3.4

Williams, E., et al. (2006), Lightning flashes conducive to the production and escape of gamma radiation to space, *Journal of Geophysical Research*, *111*(D16), doi:10.1029/2005JD006447. 3.2

Williams, E. R. (2006), Problems in lightning physics—the role of polarity asymmetry, *Plasma Sources Science and Technology*, *15*(2), S91–S108, doi:10.1088/0963-0252/15/2/S12. 4.3

Williams, E. R. (2010), The Origin and Context of C . T . R . Wilson ' s Ideas on Electron Runaway in Thunderclouds, *Journal of Geophysical Research*, *115*, doi: 10.1029/2009JA014581. 2.1

Wilson, C. T. R. (1924), The electric field of a thundercloud and some of its effects, *Proc. R. Soc. London A*, *37*, 32D–37D. 2.1, 4.1, 4.2

Wilson, C. T. R. (1925), The Acceleration of β-particles in Strong Electric Fields such as those of Thunderclouds, *Proc. Cambridge Philos. Soc.*, *22*, 534–538. 2.1, 2.2

List of abberviations

ADELE	Airborne Detector for Energetic Lightning Emissions
AGILE	Astrorivelatore Gamma a Immagini Leggero
ASIM	Atmosphere-Space Interactions Monitor
AWESOME	Atmospheric Weather Electromagnetic System for Observation, Modelling, and Education
BATSE	Burst and Transient Source Experiment
CG	Cloud to Ground (lightning)
CGRO	Compton Gamma Ray Observatory
ELF	Extremely Low Frequency
EMP	Electromagnetic pulse
GBM	Gamma-ray Burst Monitor
GRB	Gamma Ray Burst
IC	Intra cloud (lightning)
LAD	Large Area Detector
LASA	Los Alamos Sferic Array
LAT	Large Area Telescope
LIS	Lightning Imaging Sensor
LMA	Lightning Mapping Array
MCAL	Mini-Calorimeter
OTD	Optical Transient Detector
QS	Quasi electro-static
RREA	Relativistic Runaway Electron Avalanche
RFD	Relativistic Feedback Discharge
RHESSI	Reuven Ramaty High Energy Solar Spectroscopic Imager
SAMA	South Atlantic Magnetic Anomaly
STP	Standard Temperature and Pressure
TARANIS	Tool for the Analysis of Radiations from lightNIng and Sprites
TGF	Terrestrial Gamma ray Flash
TLE	Transient Luminous Event
TOGA	Time of Group Arrival
ULF	Ultra Low Frequency
UT	Universal Time
VLF	Very low Frequency
WWLLN	World Wide Lightning Location Network